An Open Access Journal available online

Covenant Journal of Physical & Life Sciences

Vol. 6 No. 1, June, 2018

A Publication of Covenant University

Editor-in-Chief: Prof. Louis Egwari
louis.egwari@covenantuniversity.edu.ng

Managing Editor: Edwin O. Agbaike
edwin.agbaike@covenantuniversity.edu.ng

Website: http//journals.covenantuniversity.edu.ng/cjpl/

ISSN: Print 2354 – 3574
Electronics 2354 – 3485

Published by Covenant University Journals,
Covenant University, Canaanland, Km 10, Idiroko Road,
P.M.B. 1023, Ota, Ogun State, Nigeria

Printed by Covenant University Press

Articles

Covenant Journal of Physical & Life Sciences (CJPL) Vol. 6 No. 1, June, 2018

An Open Access Journal available online

First Birth Interval: Cox Regression Model with Time Varying Covariates

Adeniyi O.I.[1*] & Akinrefon A.A.[2]

[1]University of Ilorin, Kwara State,
[2]Modibbo Adama University of Technology, Yola, Adamawa State
* E-mail: adeniyi.oi@unilorin.edu.ng

Abstract: The Cox regression model has been widely used for the analysis of time to event data with their associated risk factors, it assumes a constant hazard ratio over time and that the risk factors are independent of time. When the assumptions are violated, the estimates of the hazard ratio of the Cox regression estimates of the hazard ratios becomes misleading. In this study, we use a modified Cox regression model that incorporates time dependent covariate which measures the interaction of exposure with time.
Birth interval between marriage and first birth for the ever married women after marriage, taken from NDHS 2013 women data is fitted using the Cox regression model with time varying covariates due to the failure of existence of proportionality assumption. This model performs better compared to Cox regression model.
Keywords: Time to event, Hazard Ratio, Time-varying covariates, proportionality assumption

Introduction

The Cox Proportional hazard models requires that the hazard ratio is constant over time, which implies that the hazard for an individual is proportional to the hazard for any other individual, where the proportionality constant is independent of time. However, the Cox Proportional hazard model gives a misleading conclusions when the assumption is violated particularly in the presence of long follow-up period.

In order to avoid misleading estimates of the hazard ratio due to the presence of time-dependent variables, checking the proportionality of the hazards assumptions should be an integral part

of a survival analysis by a Cox regression model. Even though the Cox regression model has been widely used recent publications [1, 2 &3] suggest that the test of the validity of the assumptions must be verified before its use.

To evaluate the proportional hazard assumption, we use the residuals measures like Schoenfeld residuals [4] to whether the individual covariates pass the proportional hazard assumption and whether the model as a whole (global test) passes the assumption. Non-proportional hazards can arise if some covariate only affects survival up to sometime t or if the size of its effect changes over time. For this time varying covariates, the Cox regression model with time varying covariate is used instead of the traditional one. We illustrate our discussion with a study on birth interval between marriage and first birth for ever-married women extracted from women data, NDHS 2013.

Methodology

Cox Proportional Hazard Model

The proportional hazards model is a regression model with time to event as dependent variable. It allows inclusion of information about known (observed) covariates in models of survival analysis and is the most applied model in this area. To investigate the relation between the survival time and some risk factors called covariates, the Cox proportional hazards model is used. In this model, the relative risk is described parametrically and the hazard function is described non-parametrically. The hazard function for individual *i* is written as:

$$h(t, X_i) = \mathrm{h}_0(t)\exp(\beta X_i) \qquad 1$$

$h_0(t)$ is a baseline hazard function, left unspecified; $\exp(\beta X_i)$ is the relative risk of individual *i* with X_i as the covariate vector. In this model, covariates act multiplicatively on the baseline hazard, adding additional risks on an individual basis. Coefficient vectors of the covariates are estimated by maximizing a partial likelihood function [5]. The model parameter β are interpreted by the hazard ratio assumed to be constant over time which is given as;

$$HR = \frac{\hat{h}(t, X^*)}{\hat{h}(t, X)} \qquad 2$$

Where X^* is the set of predictors for one individual and X is the set of predictors for the other individual.

Regression models for time to event data have been based on the Cox regression model, which assumes that the underlying hazard function for any two levels of some covariates is proportional over the time. If hazard ratios vary with time, then the assumption of proportional hazards is violated, therefore methods that do not assume proportionality must be used to investigate the effects of covariates on survival time. The significance of the estimated parameter of the Cox regression model does not implies that the model is well fitted and satisfies the proportional hazard assumption and vice versa, thus, Cox proportional hazards with time varying covariates is used.

Cox Proportional Hazard Model with Time Varying Covariate

In the Cox regression model, when time-dependent variables are used to assess the proportional hazard assumption for time- independent variables, the Cox regression model

cannot be used because it can no longer satisfy the proportional hazards assumption. Therefore, Cox regression model that incorporate time-varying covariates should be used instead. A time-dependent variable is defined as any variable whose value for a given subject may differ over time (t) [6].

Given a survival analysis situation involving both time-independent and time-dependent predictor variables, the Cox proportional hazard model that incorporate both type of variables is given as

$$h\left(t,\mathrm{X}\left(t\right)\right)=h_0\left(t\right)\exp\left[\sum_{i=1}^{p_1}\beta_i X_i+\sum_{j=1}^{p_2}\sigma_j X_j g_j\left(t\right)\right] \quad 3$$

Where $\mathrm{X}\left(t\right)=\left(X_1,X_2,...,X_{p1}\right)$ are the time-independent and $\left(X_1\left(t\right),X_2\left(t\right),...,X_{p2}\left(t\right)\right)$ time-dependent variables. The term $\sigma X\left(t\right)$ is an interaction term between the covariate X and some function $\sigma\left(t\right)$ of time. The hazard ratio for Cox model with time varying covariates is given as

$$HR\left(t\right)=\frac{h\left(t,X^*\left(t\right)\right)}{h\left(t,X\left(t\right)\right)}=\exp\left[\sum_{i=1}^{p_1}\beta_i\left[X^*{}_i-X_i\right]+\sum_{j=1}^{p_2}\delta_j\left[X^*{}_j\left(t\right)-X_j\left(t\right)\right]\right] \quad 4$$

This model allows the hazard ratio to change over time giving greater flexibility than proportional hazards assumption in Eq. (2).

Likelihood estimation

Like the Cox regression model, parameters of the Cox regression model with time varying covariates can also be estimated by maximizing the partial likelihood of the model.

$$L\left(\beta\right)=\prod_{j=1}^{n}\frac{\exp\left(\beta X\left(t_j\right)\right)}{\sum_{l\in R\left(t_j\right)}\exp\left(\beta X_i\left(t_j\right)\right)} \quad 5$$

Application to data on birth interval

Dataset from the 2013 Nigeria Demographic and Health Survey (NDHS) were analysed. Data on interval of marriage to first birth were available for 26738 women aged 15-49. The survey was designed to provide these information at national, regional, and state or district levels, for both urban and rural areas. If a woman is married but has not given birth, the difference between her current age and age at marriage is used and is recorded as censored observation. We applied the methodology of Cox regression model to dataset on marriage to first birth interval (which is recorded in months).

The geopolitical zone, location of residence, religion, highest educational qualification, economic status, respondent age at marriage and working status were considered as explanatory variables. Three categories were created for Economic Status variable which comes from wealth index in NDHS data by combining 'poorest' and 'poorer' as 'poor', 'middle' are same as 'middle' and 'richer' and 'richest' are combined as rich. Also, the women's age at marriage was categorized into three arbitrary group as less than 18 years old women, 18-24 years old women and above 24 years old women. The two major religion being practiced were considered as Christianity and Islam while the highest educational qualification are categorised as No education, Primary, Secondary and Higher. The geopolitical zone in the country are North-central, North-east, North-west, South-east, South-south and South-west respectively while location of residence is classified as Urban and Rural. The working status

of the women as categories into employed and nit employed.

Checking the Proportional Hazard Assumption

To test the hypothesis that the proportion hazard assumption is the valid, the following statement of hypothesis is given;

$H_0 : \delta_1 = \delta_2 = ... = \delta_{p2}$ (Assumption is valid)

H_1 : at least one of the $\delta_i^{'}s$ is not equal to zero (Assumption not valid)

We use residual measures to investigate the departure from proportionality assumption. Schoenfeld residuals was used to test the assumption of proportional hazards. Schoenfeld residuals are usually calculated at every failure of time under the proportional hazard assumption, and usually not defined for censored observation [7, 8 & 9]. The overall significance test named as 'global test' of the model in Eq. (3) was performed from Schoenfeld residual shown in Table 1. The columns are the explanatory variables, categories of the explanatory variables, the Pearson correlation (rho) of scaled Schoenfeld residual and time (Scaled Schoenfeld residual means that it normalizes with mean from the fitted Cox regression model). The chisq is the Chi-square test of scaled Schoenfeld residual as defined by Schoenfeld in 1982 and the corresponding p-value are shown for the null-hypothesis of proportionality.

Table 1: Test of Proportional Hazard Assumption

Explanatory Variable	Categories	rho	Chisq.	p-value
Zone	North-central			
	North-east	0.0128	3.95	0.0468
	North-west	0.0725	126.84	<0.0001
	South-east	-0.0202	9.88	0.0017
	South-south	0.0006	0.01	0.9198
	South-west	-0.0245	14.57	0.0001
Location of Residence	Urban			
	Rural	0.0025	0.15	0.6951
Highest Educational Qualification	No Education			
	Primary	-0.0023	0.12	0.728
	Secondary	-0.008	1.59	0.2017
	Higher	-0.0167	6.71	0.096
Religion	Islam			
	Christianity	0.0111	3.11	0.0778
Economic Status	Poor			
	Middle	-0.0104	2.63	0.1047
	Rich	0.0014	0.05	0.8219

Working Status	Not Employed			
	Employed	0.0142	4.88	0.0272
Age at Marriage	less than 18 years			
	18 to 24 years	-0.0322	24.73	<0.0001
	Above 24 years	-0.0491	56.57	<0.0001
Global Test			909.4	<0.0001

From the p-values reported in Table 1, it was revealed that covariates zone, highest educational qualification, working status and age ta marriage showed non-proportionality character and also the global test suggested strong evidence of non-proportionality (p-value <0.0001). These numerical findings suggest a non-constant hazard ratio for these variables. Therefore, for the violation of proportional hazard assumption, a Cox regression with time varying covariate is used.

Cox Regression with time-varying covariates

We assume that $g_j(t) = t$, which implies that for each X_j in the model as main effect, there is a corresponding time dependent variable in the model of the form $X_j * t$. The Cox proportional hazard model with time varying covariate is of the form

$$h\left(t, X(t)\right) = h_0(t)\exp\left[\sum_{i=1}^{p_1}\beta_i X_i + \sum_{j=1}^{p_2}\delta_j\left(X_j * t\right)\right] \qquad 6$$

Results

Table 2 presents the parameter estimates of Cox proportional Hazard model and Cox Model with time-varying covariates. The Akaike information criterion (AIC) [10] and 2LogL was used to select the preferred model between the Cox proportional hazard model and Cox Model with time-varying covariates. The values of the selection criteria shows that Cox model with time-varying covariates is preferred. Therefore, discussion of results is upheld for the parameter estimates from Cox model with time-varying covariates.

Table 2: Parameter Estimates for Cox PH Model and Cox with Time-varying Covariates

		Cox PH			Cox with time-varying covariates					
Explanatory Variable	**Categories**	**Hazard Ratio**	**β**	**p-value**	**Hazard Ratio**	**β**	**p-value**	**Hazard Ratio**	**δ**	**p-value**
Zone	North-central									
	North-east	0.8614	-0.1492	<0.001	0.8434	-0.1703	<0.001	1.0012	0.0012	0.228
	North-west	0.7567	-0.2788	0.001	0.6147	-0.4866	<0.001	1.0072	0.0072	<0.001
	South-east	1.0628	0.0609	0.038	1.1882	0.1724	<0.001	0.9945	-0.0055	<0.001
	South-south	1.0104	0.0104	0.699	1.037	0.0363	0.343	0.9985	-0.0015	0.255

	South-west	1.2832	0.2494	<0.001	1.4023	0.3381	<0.001	0.9941	0.0059	<0.001
Location of Residence	Urban									
	Rural	0.9631	-0.0376	0.03	0.9623	-0.0384	0.027			
Highest Educational Qualification	No Education									
	Primary	1.1462	0.1365	<0.001	1.1993	0.1817	<0.001	0.9985	-0.0015	0.061
	Secondary	1.1373	0.1287	<0.001	1.2151	0.9148	<0.001	0.9968	-0.0032	0.001
	Higher	1.0706	0.0682	0.038	1.1858	0.1704	<0.001	0.9955	-0.0045	0.004
Religion	Islam									
	Christianity	0.9103	-0.094	<0.001	0.9074	-0.0972	<0.001			
Economic Status	Poor									
	Middle	1.1123	0.1064	<0.001	1.1215	0.1147	<0.001			
	Rich	1.0263	0.026	0.256	1.0392	0.03845	0.093			
Working Status	Not Employed									
	Employed	0.9941	-0.0059	0.704	0.9602	-0.0406	0.058	1.0016	0.0016	0.005
Age at Marriage	less than 18 years									
	18 to 24 years	1.1959	0.1789	<0.001	1.3711	0.3156	<0.001	0.9938	-0.0062	<0.001
	Above 24 years	0.9696	-0.0309	0.267	1.3497	0.2999	<0.001	0.9841	-0.016	<0.001
-2LogL		441976.52						441202.68		
AIC		442051.52						441232.68		

From Table 2, the results for the time varying covariates has it that the estimated hazard ratio for women for North-east

is $HR = \exp(-0.1703 + 0.0012t)$,

which implies that the estimated hazard ratio will increase exponentially by 0.0012 as the time increases compare to women form the North-central zone. Also, the hazard ratio for North-west women increases by 0.0072 as time increases while it decreases by 0.0015 and 0.0059 for women for South-south and South-west as time increases compare to women from the North-central. The hazard ratio decreases with time as the educational qualification improves by 0.0015, 0.0032 and 0.0045 for primary, secondary and higher educational qualification respectively compared to women with no formal education. The hazard ratio for employed women increases by 0.0016 as time increases compare to women who are unemployed while the hazard decreases with time by 0.0062 and 0.016 for women whose age at marriage are between 18 to 24 years and above 24 years respectively.

For the covariates that are not time varying, the hazard ratio decreases by 0.0377 for women living in the rural areas compare to women living in the urban areas. The hazard ratio decreased by 0.0926 for Christian women compare to Muslim women while the hazard increase by 0.2115 and 0.3922 for the middle and rich

economic status compare to the poor status.

Conclusion

Cox regression model been the most popular approach in analysing survival data may give misleading estimates if the underlying assumptions are validated. The power of the tests is reduced for the covariates which are not satisfying the proportionality assumption. Once it is established that the assumptions are not valid, a Cox model that incorporate time-varying covariates will give a better estimate of the parameter. From the study carried out on birth interval between marriage using dataset from 2013 Nigeria Demographic and Health Survey (NDHS), it was revealed that factors like geopolitical zone, highest educational qualification, working status and age at marriage were time-varying among other factors that were considered to affect the interval of marriage time to first birth of women. The interest of the study is to found out the covariate that are time-dependent and fit an appropriate survival model to predict the hazard ratios

References

Ata, N. A. (2007). Cox regression models with non-proportional hazards applied to lung cancer survival data. *Hacettepe Journal of Mathematics and Statistics* 36, 157-167.

Bellera, C. A. P. (2010). Variables with time-varying effects and the Cox model: some statistical concepts illustrated with a prognostic factor study in breast cancer. *BMC Medical Research Methodology* 10: 20.

Rahman, A and Hosque, R (2015). Fitting Time to First Birth Using Extended Cox Regression Model in Presence of Non-proportional Hazard. Dhaka University. *Journal of Science* 63(1): 25-30

Schoenfeld, D. (1982). Partial residuals for the proportional hazards regression model. *Biometrika* 69, 239-241.

Cox, D. R. (1972). Regression models and life-tables. Journal of the Royal Statistical Society. Series B (Methodological), 187-220.

Kleinbaum, D.G. and Klein, M. (2005). Survival Analysis: A Self-Learning Text. Springer.

Stablein, D., Carter, W., and Novak, J. (1981). Analysis of survival data with non-proportional hazard functions. *Control Clinical Trials* 2: 149–159.

Grambsch, P. M. (1994). Proportional hazards tests and diagnostics based on weighted residuals. *Biometrika* 81, 515-526.

Schoenfeld, D. (1980). Chi-squared goodness-of-fit tests for the proportional hazards regression model. *Biometrika* 67, 145-153.

Akaike, H. (1974). A new look at the statistical model identification. *IEEE Transactions on Automatic Control* 19: 716-723.

Covenant Journal of Physical & Life Sciences (CJPL) Vol. 6 No. 1, June, 2018

An Open Access Journal available online

Hepatoprotective Potential and Histological Studies of Effects of *Celosia Argentea* L. on Paracetamol-Induced Liver Damage

Dokunmu T. M.[1]* Oyelade I. F.,[2] Ogunlana O. O.,[1] Bello, O. A.,[2] Ezekiel O. M.[1] & Oladele F. W.[1]

[1]Department of Biochemistry, Covenant University,
Ota, Ogun State, Nigeria
[2]Department of Biological Sciences, Covenant University,
Ota, Ogun State, Nigeria
***** titilope.dokunmu@covenantuniversity.edu.ng

Abstract**:** *Celosia argentea* L. is a common vegetable known to possess anti-oxidative and other therapeutic properties. This study evaluates the hepatoprotective activities and histological effects of aqueous extract of *Celosia argentea* L. on acetaminophen-induced liver damage in rats, compared to the effects of a standard drug –silymarin. Twenty-five male rats were used in this study. These were divided into five groups of five animals each. Animals in group 1 were given 1ml/kg body weight (b.w) distilled water (control [C]), group 2 were given 100mg/kg b.w silymarin for 4 days plus acetaminophen for 3 days [SL], groups 3 and 4 were given 250 and 500mg/kg b.w aqueous extract of *C. argentea* for 4 days plus acetaminophen for 3 days (CA1 and CA2, respectively) and group 5 were given 1 ml/kg b.w. distilled water for 4 days and 1g/kg b.w acetaminophen (PCM) for 3 days. Serum alanine aminotransferase (ALT), aspartate aminotransferase (AST), alkaline phosphatase (ALP) and total bilirubin activities were assessed on day 8, values of mean and standard error were compared at significance level of $p < 0.05$. Overall, mean ALT, AST and ALP levels in CA2 (21.8 ± 1.4, 84.2 ± 8.2 and 175.9 ± 36.9 U/L, respectively) was lower than PCM group and similar to SL group (37.6 ± 3.9, 97.2 ± 5.2 and 151.1 ± 21.91, respectively, $p > 0.05$). Mean values in control group were similar to CA2 but significantly lower than PCM and CA1. Total bilirubin was higher but not significantly different compared to

C group, suggesting a lack of effect on total bilirubin. *C. argentea* ameliorates and protects against acetaminophen-induced liver damage in rats, with a comparable effect with silymarin at a dose of 500mg/kg b.w. A regular consumption of the vegetable can play a role in sustaining health and can be used in place of long term therapy in individuals with compromised liver or actively exposed to chemotherapeutic drugs with adverse effects on liver.

Keywords: *Celosia argentea,* liver damage, silymarin, hepatoprotective

Introduction

Liver diseases which include liver cirrhosis, fibrosis, liver cancer, hepatitis etc. are common causes of death worldwide [1] and have been linked to a number of factors which include excess alcohol intake, metabolic syndromes, hepatitis B and C infection, free radicals, overdose of non- steroidal anti-inflammatory drugs, chemicals such as carbon tetrachloride (CCl_4), halothane etc. Liver injury caused by chemicals and drugs is a major toxicological issue due to limited therapeutics for this condition without side effects. Medicinal plants have been acknowledged as a rich source of bio-actives for prevention and treatment of ailments [2]. They serve as alternative for medicines with little side effects and are good sources for development of new drugs for safe treatment of diseases.

Treatment of diseases with high doses of some drugs e.g. antibiotics, acetaminophen, methotrexate, is often associated with toxicity causing hepatic damage [3]. As a result of this shortcoming, research is directed towards discovery and use of active chemicals from medicinal plants which are commonly consumed foods that produce protective and therapeutic effects, demonstrating comparable outcomes with standard drugs and showing minimal side effects [4]. Studies are required to screen commonly consumed indigenous vegetables for their antioxidative and protective properties to serve as natural remedies for many ailing individuals. Medicinal plants have made significant contributions to the prevention and treatment of hepatotoxicity [5] one of which is *Celosia argentea.*

Celosia argentea L. is a vigorous, broad leaf, edible annual vegetable belonging to the family Amaranthaceae. It is popularly called silver cock's comb in English, *shoko* in Yoruba, Lagos spinach in Lagos, Nigeria. It is grown as edible vegetable and also for medicinal uses in Africa, Southeast Asia and other regions of the world [6]. Many bioactive compounds such as flavonoids, carotenoids, polyphenols and vitamins have been identified in *C. argentea,* which confer many biological properties due to their free radical scavenging activities [7]. Hepatoprotective properties have been reported from other regions using ethanolic extracts on CCl_4 or paracetamol-induced liver damage [7-9]. Root, stem and leaves of *C. argentea* have also been reportedly used for rapid healing of wounds, immune-stimulating, curing of kidney stones, antipyretic, antioxidant, anticancer, diuretic and antibacterial and anti-hepatotoxic effects, [10].

The aim of this study is to investigate the hepatoprotective effects of *C. argentea* L. in its edible form (aqueous

extract) on paracetamol-induced liver damage in rats and compare these effects with a standard drug – silymarin.

Materials and Methods

Plant materials: *Celosia argentea* fresh leaves were acquired from the local market at Ota in Ogun State. Plant identification was carried out by a botanist in the Department of Biological Sciences, Covenant University. The fresh leaves were washed to remove dust particles and air dried for three weeks after which they were blended into fine powder using a blender. Forty grams of the powdered leaves was put in a 500ml conical flask and 320ml of distilled water was added, and the mixture was left for 24hours and was filtered using a whatman No. 1 filter paper to obtain the filtrate. The mash obtained was again reconstituted in 320ml of distilled water and the maceration was repeated. The combined filtrate was then evaporated under reduced pressure at 80^{o}C in a rotary evaporator and the crude extract was obtained with a yield of 5g.

Experimental animals: Male albino rats with a mean weight of 140g were obtained from a commercial animal house and kept in clean cages and placed in a well- ventilated room at the animal house of the Department of Biological Sciences, Covenant University, Ogun State, Nigeria at optimum temperature and relative humidity. They were acclimatized to the laboratory condition for one week and were given food and water *ad libitum*. All animals were treated in accordance with the recommendations of National Institute of Health (NIH) guidelines for the care and use of laboratory animals [11].

Study groups: The rats (n = 25) were divided into 5 groups of five animals in each group. The animals in group 1(C) served as normal control group and were given only vehicle (distilled water, 1ml/kg b.w.) for 7 days, animals in group 2(SL) served as positive control and were given Silymarin (100mg/kg b.w.) for 4 days and PCM for 3 days, group 3(CA1) and 4(CA2) received 250 and 500mg/kg b.w aqueous extract of *C. argentea* respectively for 4 days plus paracetamol on days 5 – 7. Group 5 (PCM) served as the negative control and were administered with only vehicle (1ml/kg b.w.) for 4 days plus paracetamol (1g/kg b.w.) on days 5 – 7.

Blood collection and preparation of tissue sample: Animals were anaesthetized 24hours after the last treatment on the 7th day with diethyl ether prior to dissection and blood samples were collected through cardiac puncture into lithium heparinized bottles for aspartate aminotransferase (AST), alkaline phosphatase (ALP), alanine aminotransferase (ALT) and total bilirubin (TB) assays. Serum was obtained by centrifuging the blood at 4000 rpm for 15 minutes into 2ml tubes and stored at -20^{o}C until required for the assays. The liver was excised and washed in normal saline (0.9% NaCl) and a portion fixed in 10% formaldehyde for histopathological examination.

Analysis of biochemical parameters: Commercial test kits for AST, ALT, ALP and total bilirubin (Randox® Laboratories, United Kingdom) were purchased and used for liver function tests following the protocol from the

supplier's specifications from the standard kits.

Histological analysis: A section of the liver was fixed in 10 % formalin immediately after sacrifice. The fixed liver sections were embedded in paraffin, 5-6µm thick liver section was stained in hematoxylin-eosin; this was examined under compound microscope for determination of histopathological changes

Statistical analysis

Data is presented as mean ± standard error of mean (SEM) for continuous data and was compared using one way ANOVA followed by Least square difference (LSD) post hoc test, all test of significance was taken at $p<0.05$.

Results

Twenty five healthy animals with mean weight of 140g on day 0 were used for the experiment. There was no significant difference in the weight of the animals after treatment on day 7 ($p>0.05$). There was also no change in the physical appearance of the animals.

Effects of treatment on liver function tests

The mean values of 2 doses of *Celosia argentea* on serum alkaline phosphatase, aspartate aminotransferase, alanine aminotransferase and total bilirubin in the experimental animals are shown in figures 1 - 4. There was a significantly higher serum AST level in group CA1 105.18±7.26 U/L, this was similar to group PCM with mean value of 113.11±6.20 compared to control group with a mean value of 84.58±11.22 ($p<0.05$). The corresponding mean and SEM values in group CA2 (84.21±8.25) was similar to SL (97.24±5.23) and control. Figure 1 shows the serum AST levels in all groups after treatment.

There was also a significantly higher serum ALP level in group PCM with a mean value of 385.02±38.62 compared to the control group with a mean value of 128.34±20.7 U/L, indicating liver damage. Animals in group SL, CA1 and CA2 had significantly lower mean values of 151.11±29.92, 226.32±33.67 and 175.95±36.94U/L respectively. Mean values of groups SL and CA2 were similar ($p>0.05$). Figure 2 shows the ALP levels in all groups after treatment.

Similarly, there was a significantly higher serum ALT level in group PCM with a mean value of 55.40±3.48 U/L. The corresponding values in Groups SL, CA1 and CA2 are 37.60±3.93, 30.00±5.69 and 21.80±1.49 U/L respectively. The result is shown in figure 3. There was no significant change in the total bilirubin of the animals in groups CA1 and CA2 suggesting that the plant has no significant effect on total bilirubin (figure 4).

Histological analysis

The liver of control rats (figure 5) showed hepatocytes arranged in plates, a fibrocollagenous connective tissue stroma without necrosis or any area of infiltration by lymphocytes. This is in contrast with the features observed in the animals in group PCM (figure 6) that shows infiltration of the portal tracts and interface by lymphocytes (Portal & Interface Hepatitis), presence of necrosis within which are cellular debris, extensive bile regurgitation i.e. cholestasis and bile ductular proliferation. However, the animals in groups CA1 (figure 7) showed infiltration of portal tracts with small areas of necrosis while animals in groups CA2 (figure 8) and SL (figure 9) showed similar features of

infiltration of portal tracts without any areas of necrosis.

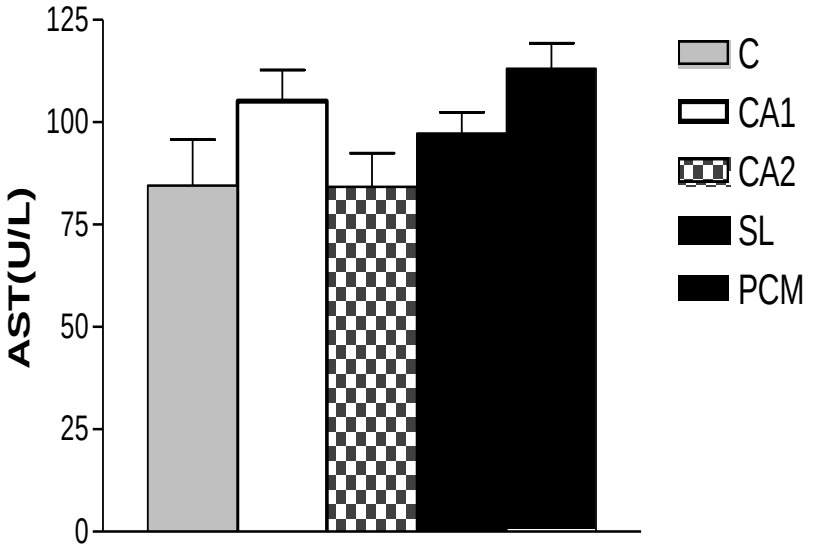

Figure 1: Histogram showing changes in AST mean values (with SEM) in the experimental animals after treatment

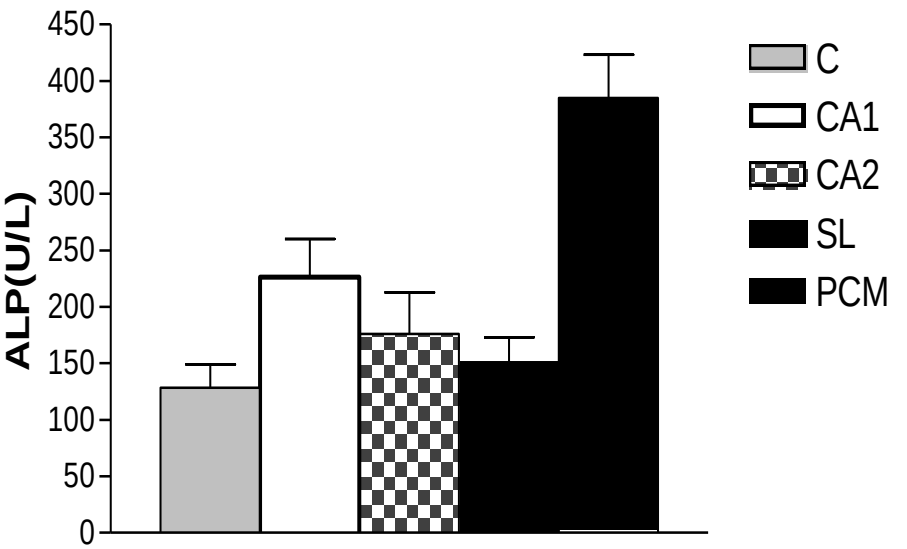

Figure 2: Histogram showing changes in ALP mean values (with SEM) in the experimental animals after treatment

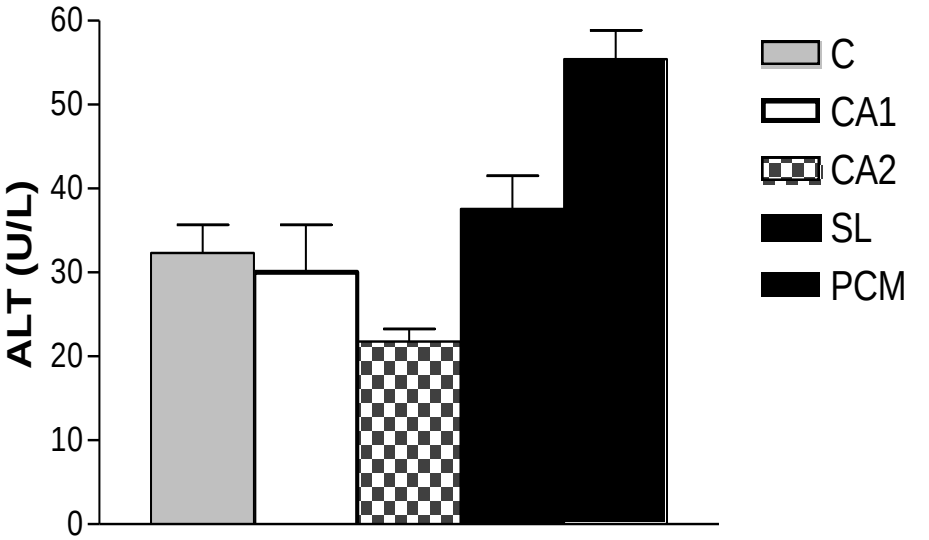

Figure 3: Histogram showing changes in ALT mean values (with SEM) in the experimental animals after treatment

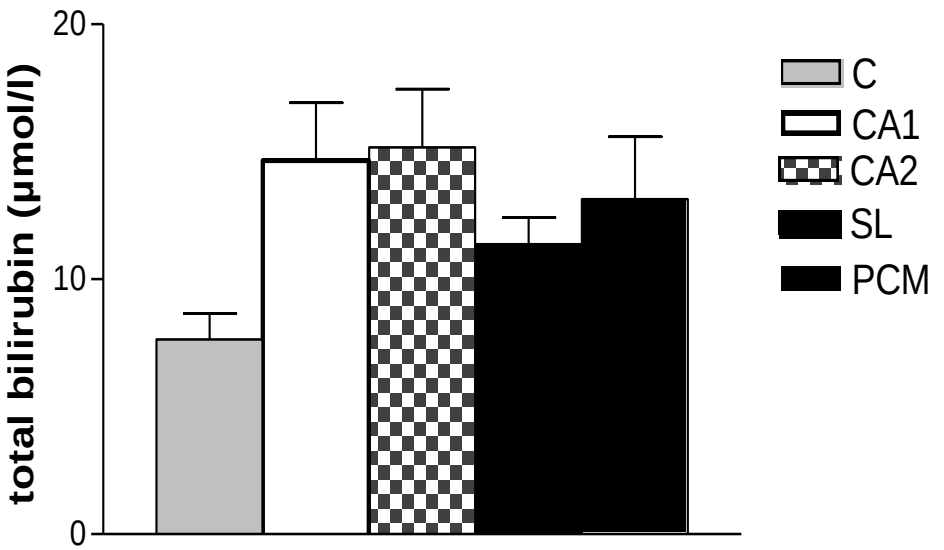

Figure 4: Histogram showing changes in total bilirubin mean values (with SEM) in the experimental animals after treatment.

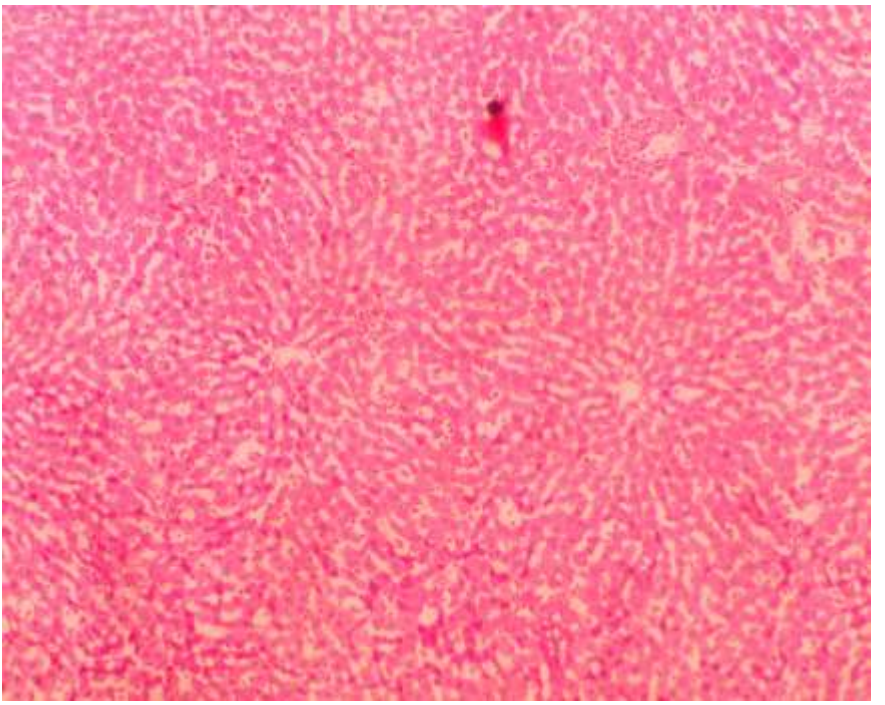

Figure 5: Control group showing hepatocytes (light arrow) arranged in plates within a fibrocollagenous connective tissue stroma (Haematoxylin & Eosin stain, x 40 magnification).

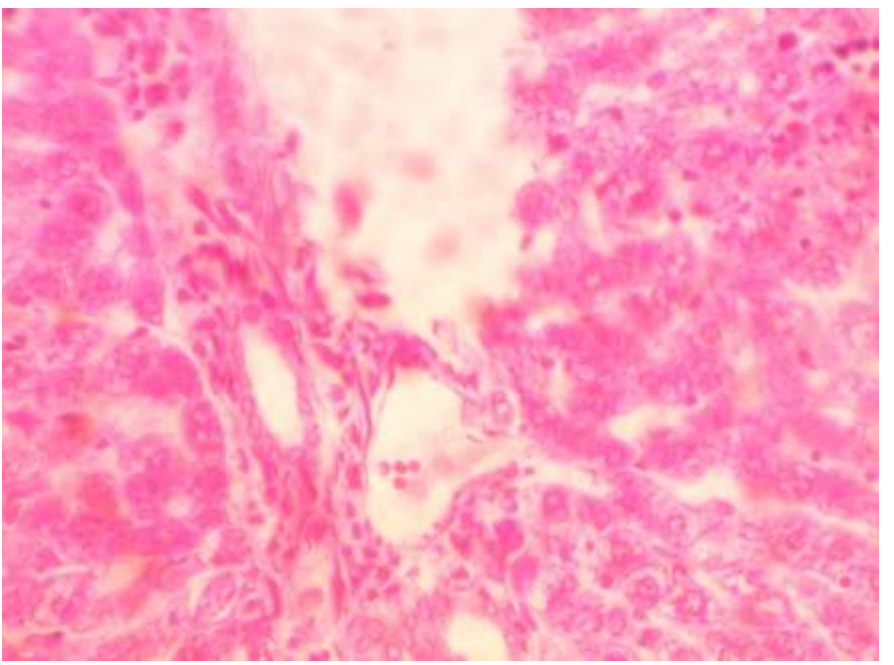

Figure 6: PCM group showing bile ductular proliferation (light arrows) within the portal tract (Haematoxylin & Eosin stain, x 100 magnification)

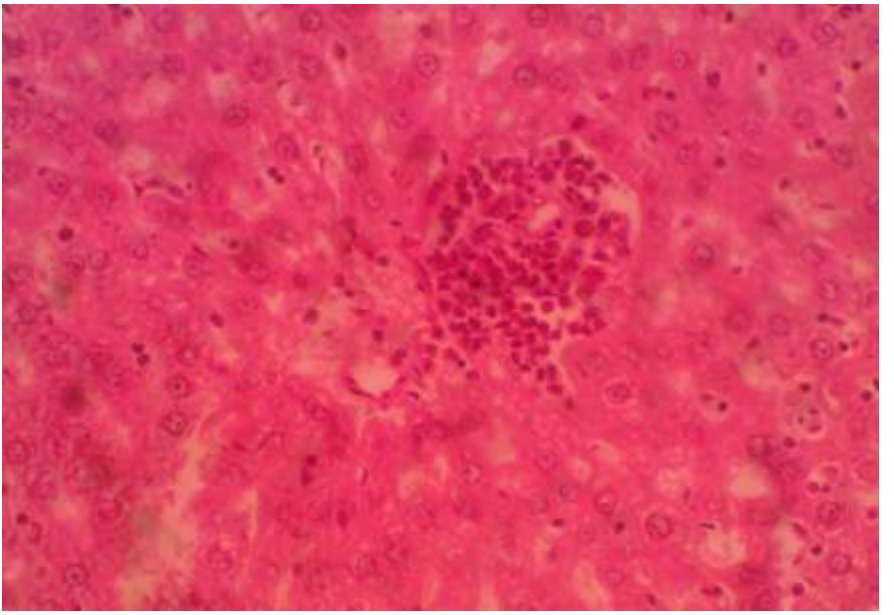

Figure 7: CA1 showing lymphocyte aggregation (light arrow) in the interface (Haematoxylin & Eosin stain, x 100 magnification).

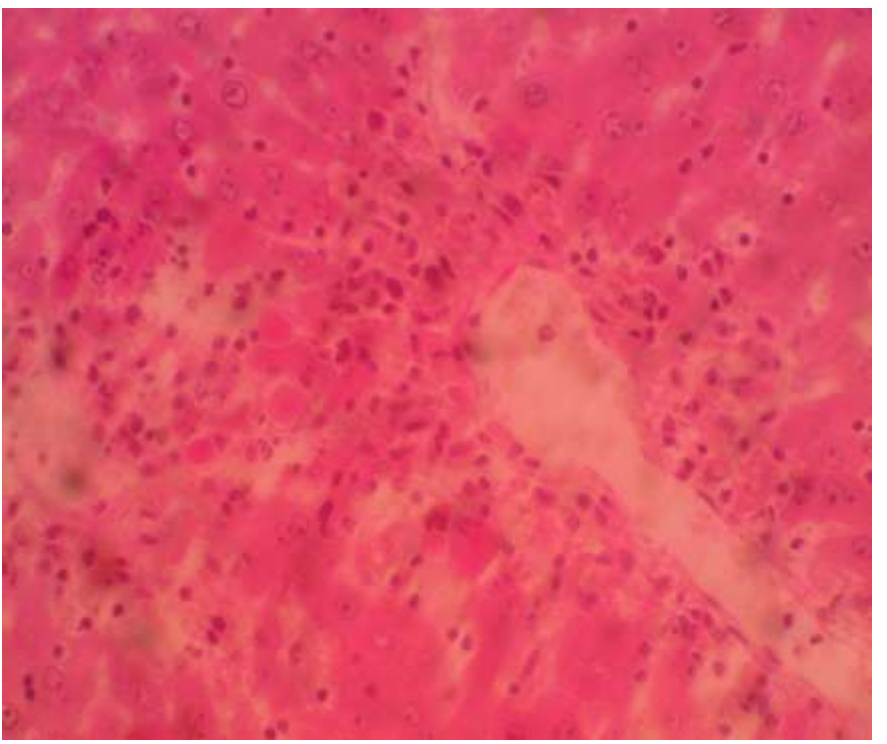

Figure 8: CA2 showing florid lymphocyte infiltration (light arrow) within the interface {interface hepatitis} (Haematoxylin & Eosin stain, x 100 magnification).

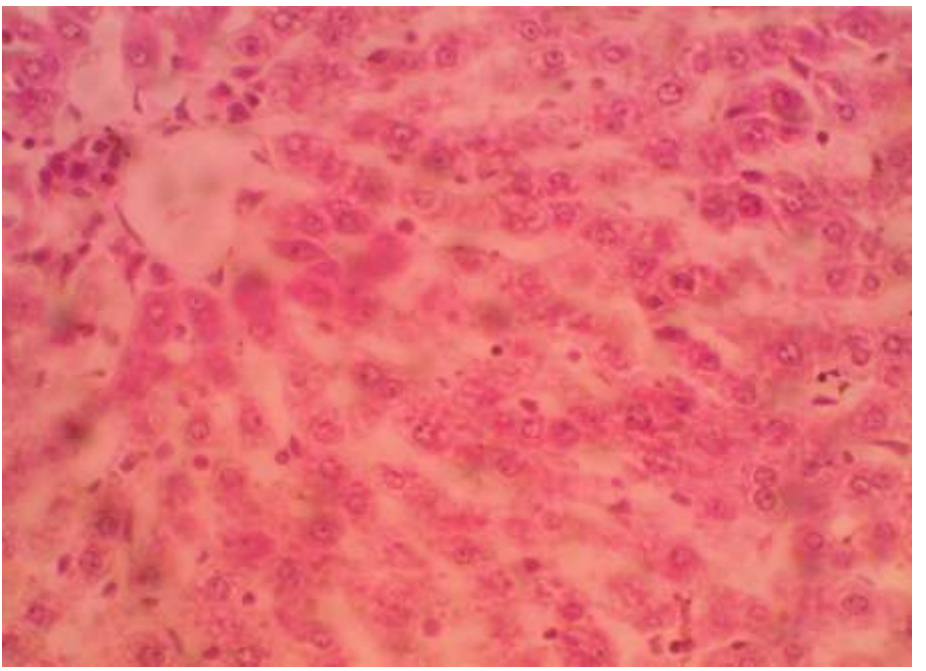

Figure 9: Silymarin group showing infiltration of lymphocytes (light arrow) within the interface {interface hepatitis} (Heamatoxylin & Eosin stain, x 100 magnification).

Discussion

Medicinal plants have been acknowledged as a rich source of bio-actives for prevention and treatment of ailments [2]. The ability of any medicinal plant to ameliorate harmful effects or restore physiologic state of hepatocytes after exposure to a hepatotoxic agent makes it a hepatoprotective plant. The results obtained from this study is in conformity with induced liver damage previous literatures with overdose of acetaminophen [12-13] as evidenced by the increased activities of serum ALT, ALP, AST and total bilirubin compared to animals that were not treated with the toxic doses of the drug. Acetaminophen-induced liver damage is marked by hepatocellular necrosis and leads to an increase in the activities of serum ALT, AST, ALP and total bilirubin [14]. The increased level of serum ASP and ALT indicates loss of functional integrity of liver cell membrane and cell leakage and ALP is related to functioning of the hepatocytes and its increased level in the serum indicates obstructive jaundice and intra-hepatic cholestasis [15].

Liver is a vital organ of the body that plays important roles in metabolism of xenobiotics, endogenous compounds, and is involved in many biochemical processes thus receives the most toxicological assault resulting from oxidative stress. Necrosis of the liver cells is one of the most common effects of paracetamol toxicity [16]. The pathogenesis of liver damaged has been shown to be due to highly

reactive metabolite, N-acetyl-p-benzoquinone imine (NAPQ1) formed in excess as well as other oxidants e.g. nitric oxide which covalently binds to cysteine residues of proteins to form adducts, in hepatic centrilobular cells that develop into necrosis [17]. This occurs in the presence of oxidative stress.

Oxidative stress, a condition in which there is an imbalance between the concentrations of reactive oxygen species (ROS) and physiological antioxidants, resulting in oxidative damage to many biomolecules within the cell. It is well established as a major risk factor for the development of several diseases including atherosclerosis, liver diseases, cardiovascular disease, cancer, etc. The histology results of the liver in acetaminophen treated animals showed necrosis, infiltration of portal tracts by inflammatory cells, cholestasis. However animals pre-treated with 500mg/kg aqueous extract of *C. argentea* were protected against necrosis by acetaminophen. The biochemical assays also corroborate this finding showing reduced serum ALT, AST and ALP activities in CA2 group. The results are in agreement with previous studies which reported that ethanolic extracts of *Celosia argentea* seeds or plant exhibited similar hepatoprotective activity against carbon tetrachloride-induced and paracetamol-induced hepatotoxicity in rats [8-9].

Silymarin, a flavonoid containing drug is known to protect against liver diseases [13, 18] at a dose range of 25 to 200mg/kg b.w. The hepatoprotective effect of *C. argentea* was demonstrable at a dose of 500mg/kg b.w and this was similar to effects observed in silymarin group, however there was very limited effect when administered at 250mg/kg b.w. Leaf extract of *C. argentea* contains phytochemicals such as alkaloids, saponins, flavonoids and tanins [9, 19]. These hepatoprotective potentials are indeed due to abundant phytochemicals in the plant but studies are needed to determine the actual or combination of phytochemicals responsible for the hepatoprotective activity observed.

This in turn can be increased in newly developed drugs to enhance their activities.

It can be concluded from our studies that *Celosia argentea* has hepatoprotective property in a dose-dependent manner and with comparable effect with silymarin, a standard drug for treating liver diseases. It is highly recommended that *Celosia argentea* should be included regularly in diets for prevention of liver diseases and toxicity of the liver because of the proven health benefits. It is also readily available as an indigenous vegetable that is relatively cheap and shows no toxic effects compared to treatment with standard drugs.

References

1. World Health Organisation (2016). Global health estimates 2015: Deaths by cause, age, sex, by country and by region, 2000-2015. Geneva, Switzerland: World Health Organisation.

2. Varsha, K., Amit, K. N. and Abhinav, A. (2011). Hepatoprotective prospective of herbal drugs and their vesicular carriers– a review. *International Journal of*

Research in Pharmaceutical and Biomedical Sciences 2: 360-374.

3. Mehta, N., Ozick, L. A. and Gbadehan, E. (2016). Drug-induced hepatotoxicity. (Ed) Pinsky, M. R. Available at http://emedicine.medscape.com /article/169814-overview
4. Salama, S. M., Abdulla, M. A., Alrashdi, A. S., Alkiyumi, S. S. and Golbabapou, S. (2013). Hepatoprotective effect of ethanolic extract of *Curcuma longa* on thioacetamide induced liver cirrhosis in rats. *BMC Complementary and Alternative Medicine* 13(1): 56.
5. Manoj, S., Mohanty, P. K. and Jaliwala, Y. A. (2011). Hepatoprotective activity of fruits of *Prunus domestica*. *International Journal of Pharmacy and Biological Science* 2: 439–453.
6. Yarger, L. (2007). Lagos Spinach. ECHO Technical Note. Available at www.echonet.org. *Retrieved 29th May 2017*
7. Surse, S. N., Shrivastava, B., Sharma, P., Gide, P. S. and Sana, A. (2014). *Celosia cristata*: Potent pharmacotherapeutic herb – A review. *International Journal of Pharmaceutical and Phytopharmacological Research* 3: 444-446
8. Jain, G. C. (2005). Hepatoprotective activity of ethanolic extract *Celosia argentea* Linn. Seeds in rats. *Journal of Phytochemical Research* 18: 87-90.
9. Haribabu, S. and kumaAdupa, S. (2014). Phytochemical screening and hepatoprotective activity of *Celosia argentea* Linn. *Journal of Pharmacy Research* 8(3): 405-409
10. Rajni, B. R. and Deokule, S. S. (2013). Pharmacognostic and phytochemical investigation of *Celosia argentea* Linn. *International Research Journal of Pharmacy* 4(6): 138-144.
11. National Institute of Health (1985). Guide for the care and use of laboratory animals. US. Department of Health Education and Welfare. NIH Publication No. 85-123.
12. Arumugam, A., Gunasekaran, N. and Perumal, S. (2015). Hepatoprotective effect of leaf extracts from *Citrus hystrix* and *C. maxima* against paracetamol induced liver injury in rats. *Food Science and Human Wellness* 4: 35–41.
13. Sabiu, S., Sunmonu, T. O., Ajani, E. O. and Ajiboye, T. O. (2015). Combined administration of silymarin and vitamin C stalls acetaminophen-mediated hepatic oxidative insults in Wistar rats. *Revista Brasileira de Farmacognosia* 25: 29–34.
14. Yousef, M. I., Omar, A. M., El-Guendi, M. I. and Abdelmegid, L. A. (2010). Potential protective effects of quercetin and curcumin on paracetamol-induced histological changes, oxidative stress, impaired liver and kidney functions and haematotoxicity in rat. *Food and Chemical Toxicology* 48(11): 3246–3261.
15. Adebayo, A. H., Abolaji, A. O., Kela, R., Oluremi, S. O., Owolabi, O. O. and Ogungbe,

O. A. (2011). Hepatoprotective activity of *Chrysophyllum albidum* against carbon tetrachloride induced hepatic damage in rats. *Canadian Journal of Pure and Applied Sciences* 5(3): 1597-1602.

16. **Bessems, J. G**. and **Vermeulen, N. P**. (2001). Paracetamol (acetaminophen)-induced toxicity: molecular and biochemical mechanisms, analogues and protective approaches. ***Critical Review in Toxicology*** 31(1): 55-138.
17. Roberts, D. W., Bucci, T. J. and Benson, R. W. (1991). immunohistochemical localization and quantification of the 3-(cysteine-s-yl)-acetaminophen protein adduct in acetaminophen toxicity. *American Journal of Pathology* 138: 359-371.
18. Feher, J. and Lengvel, G. (2012). Silymarin in the prevention and treatment of liver diseases and primary liver cancer. *Current Pharmaceutical Biotechnology* 13: 210–217.
19. Okpako, E. and Ajibesin, K. (2015). Antimicrobial Activity of *Celosia argentea* L. Amaranthaceae. *American Journal of Research Communication* 3(5): 123-133.

Covenant Journal of Physical & Life Sciences (CJPL) Vol. 6 No. 1, June, 2018

An Open Access Journal available online

Itaconic Acid Production from Date Palm (*Phoenix Dactylifera L*) Using Fungi in Solid State Fermentation

Ajiboye A. E.,[1]* Adedayo M. R.,[1] Babatunde S. K.,[1] Odaibo D. A.,[2] Ajuwon I. B.[1] & Ekanem, H. I.[1]

[1]College of Pure and Applied Sciences,
Department of Biosciences and Biotechnology,
Kwara State University, Malete, P.M.B. 1530, Ilorin,
Kwara State, Nigeria.
[2]University of Ilorin Teaching Hospital,
Ilorin, Kwara State. Nigeria
*adeyinka.ajiboye@kwasu.edu.ng; lizzyboye@hotmail.com

***Abstract*:** This study evaluates the potentials of *Phoenix dactylifera L* (Date fruits) as possible alternative raw materials for itaconic acid production using naturally occurring fungi. Date fruit (pulp) was used as a substrate in solid state fermentation for the production of itaconic acid using naturally occurring fungus.The date fruit (pulp) was de-capped from its seed manually with the aid of a knife and dried in an oven at 60 ^{0}C and was grounded using an Excella Mixer grinder. The fungus used was naturally isolated by fermentation of substrate (date pulp) and was identified as *Aspergillus niger*. Proximate analysis was carried out on the substrate using standard methods. Parameters such as substrate concentration, inoculum size and fermentation period were varied using standard methods to determine its effect on itaconic acid production. Assay for itaconic acid production was carried out using standard methods at a wavelength of 385nm. Amount of itaconic acid produced was derived by translation of absorbance values on the itaconic acid curve. The substrate had a high carbohydrate content of 72.29%. The fermentation results showed maximum production of itaconic acid of 20.75±0.25mg/ml using 40g substrate, 15.13±1.13mg/ml using 2 ml inoculums size of spore suspension (2×10^5 spores/ml) and a maximum yield of 16.88±0.13mg/ml at day 1 of

fermentation period. On optimization with 40g substrate and 2 ml inoculums for 3 days a maximum yield was observed at day 2 of fermentation with a maximum yield of 25.00±1.00mg/ml. The highest acidic level throughout the fermentation period was observed to be at pH 4.2. From the study it was concluded that date pulp is a promising substrate and could be utilized by *Aspergillus niger* for the production of itaconic acid.

Keywords*:* Phoenix dactylifera L *solid state fermentation, itaconic acid,* Aspergillus niger

Introduction

Organic acids have diverse applications in various fields especially in the industries. They include lactic acids, citric acid, gluconic acid and itaconic acid manufactured by large-scale bioprocesses [1]. Among them, the Itaconic acid (methylene succinic acid) is one of the most prominent one. It is a colorless, crystalline carboxylic acid obtained by the fermentation of polysaccharides [2]. Various microorganisms such as fungi of the genus *Aspergillus* have been employed in itaconic acid production through fermentative processes [3]. The most prolific producer being *Aspergillus terreus* which has been frequently utilized for itaconic acid production and subjected to grow under phosphate-limited conditions [4, 5] In the industrial production of itaconic acid, the culture medium is optimized for optimum production and the carbon source mainly used is glucose or sucrose which is readily available [6]. Other species of *Aspergillus* such as *A. niger* has also been employed for itaconic acid production. Itaconic acid is applied primarily in the polymer industry where it is employed as a co monomer for certain products [1]. Its derivatives are used in medicine and cosmetic preparation. The polymerized esters of itaconic acid are used as adhensives, coatings plastics, and elastomers [7]. An N-vinylcaprolactam-containing copolymer of acrylic itaconic acid [8] and poly (acrylic acid-co-itaconic acid) [9] was developed to be used in mechanical and functional GICs. These products are increasingly used in clinical dentistry [10].

The biosynthesis of itaconic acid was not understood for a long time because it was not certain whether itaconic acid emanated from the tricarboxylic acid (TCA) cycle or from a different pathway via citramalate or the transition step via the condensation of acetyl-CoA [11-13]. Bentley and Thiessen [14] suggested a pathway for the biosynthesis of itaconic acid; the breakdown of glucose to pyruvate via glycolysis. This pathway was confirmed by tracer experiments with ^{14}C and ^{13}C labeled substrates [14-16]) and also the necessary enzymatic activities have been proposed [11, 15]. In recent times, itaconic acid was detected in mammalian cells, where it was found in macrophage-derived cells [16]. However, no specific gene encoding this enzymatic activity has been identified and its hysiological role in mammalian cells is still unknown. According to the studies of [16] there are speculations on the role of itaconic acid as an inhibitor of metabolic pathways, because it is described as an enzymatic inhibitor.

Itaconic acid is widely employed to prepare resins used in emulsions coating, leather coating, coatings for car, refrigerators and other electrical appliances to improve adhesion, color and weather resistance [2]. Thus the need to produce itaconic acid attracts much attention. Various agro-industrial wastes can be fermented for the production of itaconic acid. Date palm (*Phoenix dactylifera* L) a tropical and subtropical tree, belonging to a family Palmae (Arecaceae) is one of the oldest plants cultivated. There is an alarming increase in the worldwide production, utilization and industrialization of dates [17]. Many date fruit producing countries are increasing its production annually. Date fruit have potential for use in production with economical advantages [18]. Date fruits have high nutritional value due to their high sugar content (around50–60%), potassium (2.5 times more than bananas), calcium, magnesium and iron as well as vitamins B_1 & B_2 and Niacin. Furthermore, dates are rich in the monosaccharides: glucose and fructose. Date fruits are considered as very nutritious and they contribute to human health especially when consumed with other food constituents [19, 20]. In Solid-state fermentation (SSF), microorganisms grow on solid materials without the presence of free liquid [21], the process occurs in absence or near absence of free water by employing a natural substrate or inert substrate as carbon source and solid support [22]. Date pulp has potentials for use in industries for acid production with economic advantages. However at the point of transportation, due to mechanical damage during harvesting or mishandling fruit may spoil or may be damaged making it unsuitable for consumption and this damaged fruits instead of being a waste can be made useful in an industrial process. Hence this study is designed towards total utilization of date fruit (date pulp) for the fermentative production of itaconic acid. Scope for value addition using bioprocessing, fermentation with microorganism and increasing yield of itaconic acid by varying various parameters needed to obtain maximum production of itaconic acid.

Materials and Methods

Sample collection and preparation: Date fruit was bought from Zango area in Ilorin, Kwara State. The fruit was identified at the Plant Biology Department, University of Ilorin, Nigeria as *Phoenix dactylifera. L* The pulp was separated from the seed manually with the aid of a knife, pulp was oven dried at 60 ^{0}C and was ground to powder using an Excella mixer grinder and preserved in an airtight container.

Isolation and preservation of test organism: Date fruit (*Phoenix dactylifera L*) pulp was subjected to natural fermentation. Ten grams of grinded fruit pulp substrate was put in a sterile plastic container and mixed thoroughly with 10 mls of distilled water. A clean muslin cloth was then used to cover the plastic for fermentation to take place for 7 days at 28 ^{0}C [23, 24]. After 5 days, 1g of fermented substrate was weighed, serial dilution was carried out and 1 ml of the dilutions was plated out. The isolated fungus was characterized and identified macroscopically and microscopically [25, 26, 27] as *Aspergillus niger*.

Preparation of spore suspension: Wild type *Aspergillus niger* was grown on sabouraud dextrose agar slant at 28 ^{0}C for 7 days. The spore inoculum was prepared by adding 3 ml of sterile distilled water to each slant containing the cultured fungi and slants were shook for one minute. Number of spores was counted to be 2×10^5 spores/ml [28].

Preparation of fermentation salts: To four conical flasks containing 100 ml of distilled water each, 0.1g of (0.25% (w/v) NH_4cl, 0.095% (w/v) KH_2PO_4, 0.0088% (w/v) $MgSO_4$, and 0.0004% (w/v) $CUSO_4$) was weighed into each conical flask respectively and was stored in an airtight bottle prior to use.

Preparation of bromine reagent: One milliliter of bromine, 3.00g of potassium bromide, 1.87g of potassium chloride, 48.50 ml of 1N hydrochloric acid, and 500 ml of water was used in the preparation of the bromine reagent as used by Fredkin [29]; El Imam *et al.* [30]. Reagent was preserved in an amber reagent bottle.

Solid state fermentation: Varying grams of dried and grinded date pulp was weighed into a 250 ml Erlenmeyer flask, 2 ml of each salts (0.25% (w/v) NH_4cl, 0.095% (w/v) KH_2PO_4, 0.0088% (w/v) $MgSO_4$, and 0.0004% (w/v) $CUSO_4$) were added. Water was added according to varying substrate water holding capacity. Flasks were corked with cotton wool wrapped with foil paper. Flasks were sterilized in an autoclave at 121 ^{0}C for 15 minutes and were allowed to cool. On cooling, substrates were inoculated with spore suspension of *Aspergillus niger* and incubated at 28 ^{0}C. One gram of sample was taken on daily basis to assay for production of itaconic acid using a spectrophotometer.

Assay for itaconic acid: Into a 3 ml curvette, was dispensed 0.3 ml of bromine reagent using a micropipette and was made upto 1.0 ml with distilled water, HCl at pH 1.2 was added to make upto 3.0 ml and left for 15 minutes. After 15 minutes spectrophotometer was blanked at 385nm. Into another 3 ml Beckman cuvette was added 0.3 ml of bromine reagent using a micropipette, 1.0 ml of sample and HCl at pH 1.2 to a volume of 3.0 ml. After 15 minutes the change in optical density was read at 385nm, wavelength of maximum absorption of bromine was also read. Readings were repeated in 20 minutes to ascertain that reaction is completed (Friedkin, 1945).

Proximate analysis of Date pulp (*Phoenix dactylifera. L*): Determination of moisture content, ash content, crude protein content, crude lipid content, crude fibre and total carbohydrate content were determined according to the method of A.O.A.C [31]

Optimization of parameters used during the period of fermentation: The optimum conditions during fermentation were determined by varying parameters such as period of incubation (fermentation days), substrate concentration and inoculum size.

***Effect of varying fermentation days*:** Fermentation days were varied for ten days. Twenty gram of substrate (Date pulp powder) was weighed into ten 250 ml Erlenmeyer flasks and this process was carried out in duplicates. 2 ml of each Salts (0.25% (w/v) NH_4cl, 0.095% (w/v) KH_2PO_4, 0.0088% (w/v) $MgSO_4$, and 0.0004% (w/v) $CUSO_4$) were added and 20 ml of distilled

water was added to the content in flasks. Flasks were cotton plugged and autoclaved at 121 ^{0}C for 15 minutes. They were inoculated with 2ml of spore suspension and were incubated at 28 ^{0}C for 10 days. pH readings and assay for itaconic acid were carried out in duplicates on a daily basis.. One gram of the substrate was dissolved in 100 ml of distilled water and filtered using a Whatman filter paper. Filtrate was used to assay for production of itaconic acid at 24 hours interval. Quantity of itaconic acid was derived by translating from the itaconic acid curve.

***Effect of varying inoculum size*:** Twenty grams of substrate (Date pulp powder) was weighed into 250 ml Erlenmeyer flasks. Twenty milliliters of distilled water was added, cotton plugged and autoclaved at 121 ^{0}C for 15 minutes. After cooling, the flasks were inoculated with 1, 2, 3, 4, 5, and 6 ml of spore suspension (2×10^5 spores/ml) of *A. niger* incubated at 28 ^{0}C for 6 days. They were assayed for itaconic acid on a daily basis as described above

***Effect of varying substrate concentration*:** Different substrate concentrations of the date fruit pulp were also analysed by weighing 10, 15, 20, 25, 30, 35 and 40g of the substrate into 250 ml Erlenmeyer flasks. Fermentation salts were added along side with distilled water according to varying water holding capacity. Flasks were sealed and autoclaved at 121 ^{0}C for 15 minutes and were allowed to cool. After cooling 2 ml of spore suspension (inoculum) was added to each flask and flasks were incubated at 28 ^{0}C for 6 days. Daily pH readings and assay for itaconic acid were carried out as described above. Filtrate was used to assay for production of itaconic acid at 24 hours interval. Quantity of itaconic acid was derived by translating from the itaconic acid curve.

Statistical analysis: The data obtained was analyzed statistically using one way ANOVA. Post-Hoc test using the Duncan Multiple Range test (DMRT) was used to test for the means that are significantly different from each other. A level of significance was determined at $p<0.05$. Statistical package (SPSS 20) was used.

Results

The results as shown in these study shows that Date fruit (pulp)(*Phoenix dactylifera. L*) have the tendency of being used as a substrate in the production of Itaconic acid through solid state fermentation by naturally occurring *Aspergillus niger* isolated from the natural fermentation of Date pulp (*Phoenix dactylifera. L*). Table 1 shows the proximate composition of Date pulp (*Phoenix dactylifera. L*).

Proximate composition of Date pulp

The proximate composition of Date pulp (*Phoenix dactylifera. L*) as shown in Table 1 depicts that carbohydrate have the highest value of 72.29% and Ash content have the lowest value of 2.00%.

Effect of varying fermentation period on itaconic acid production by *Aspergillus niger*

The effect of varying fermentation period of Date pulp for the production of Itaconic acid by naturally occurring *Aspergillus niger* are presented in Table 2. In the fermentation, Date pulp showed the highest yield of 16.88±0.13mg/ml of itaconic acid at day 1followed by day 2 which had a yield of 15.38±0.38mg/ml of itaconic acid and had the lowest yield of

12.75±0.75mg/ml of itaconic acid on day 9.

Effects of varying inoculum size on itaconic acid production by *Aspergillus niger*

The effect of varying inoculum size of Date pulp for the production of Itaconic acid by naturally occurring *Aspergillus niger* are presented in Table 3. In the fermentation, 2 ml showed the highest yield of 15.13±1.13mg/ml of itaconic acid at day 6 and had the lowest yield of 12.00±0.00mg/ml on day 2 of fermentation.

Effect of varying substrate concentration on itaconic acid production by *Aspergillus niger*

The effect of varying substrate concentration of Date pulp for the production of Itaconic acid by naturally occurring *Aspergillus niger* are presented in Table 4. In the fermentation, 40g of the substrate showed the highest yield of 20.75±0.25mg/ml of itaconic acid at day 1 followed by day 2 which had a yield of 18.88±0.13mg/ml and had the lowest yield of 14.88±0.13mg/ml on day 4.

Optimum production of itaconic acid by *Aspergillus niger* using Date pulp (*Phoenix dactylifera L*)

Optimum production of itaconic acid from all the fermentation parameters by *Aspergillus niger* was carried out with 40g substrate, 2 ml of inoculum size for 3 days at 28 ^{0}C for maximum yield of Itaconic acid and this is shown in Table 5. In the fermentation, day 2 showed the highest yield of 25.00±1.00mg/ml of itaconic acid and there was a decrease in day 1 and 3.

pH values of varying the fermentation period of the fermenting substrate by *Aspergillus niger*

The pH of the fermenting substrate for the fermentation period was taken at an interval of 24 hours. Figure 1 shows the chart representing the fermentation period and as observed the highest acidity was observed to be at pH 4.3.

pH values of varying inoculum size of the fermenting substrate by *Aspergillus niger*

The pH of the fermenting substrate for the inoculum size was taken at an interval of 24 hours. Figure 2 shows the chart representing the inoculum sizes with highest acidic level of pH 4.2.

pH values of varying the substrate concentration of the fermenting substrate by *Aspergillus niger*

The pH of the fermenting substrate for the substrate concentration was taken at an interval of 24 hours. Figure 3 shows the chart representing the substrate concentration with highest acidic level of pH 5.4.

Discussion

The results as shown in this study show that Date pulp (*Phoenix dactylifera L*) have the tendency of being used as a substrate in the production of Itaconic acid through solid state fermentation by naturally occurring *Aspergillus niger* isolated from the natural fermentation of Date pulp (*Phoenix dactylifera L*). The proximate composition of Date pulp reveals that carbohydrate content was highest while the Ash content had the lowest value (Table 1). The high carbohydrate content in the pulp serves as a source of sugar to be utilized by the fungi in the fermentation process for optimum production of itaconic acid. This agrees with earlier reports of the importance of polysaccharides in

fermentation [32, 33]. However, carbohydrates that are easily metabolized have been found essential for good production of organic acid [34]. Naturally occurring fungi, *Aspergillus niger* growing on fermented Date pulp have the potential of producing itaconic acid which can be used in industries. This is similar to the work of Ajiboye and Sani [35], that *A. niger* was one of the naturally occurring fungus during fermentation of *Dialium guineense* for citric acid production. However *Aspergillus terreus* still remains the main producer of itaconic acid [1].

Varying of fermentation period showed gradual decrease by every 24 hours. As shown in Table 2, it was observed that day 1 had the highest yield of itaconic acid while day 9 had the lowest yield. This could be due to oxygen and nutrient depletion, more so it could be due to the gradual decrease in the amount of sugar present in the fermenting medium as the fermentation process progresses. The difference in the sugar content and surface area of the starting materials for the fermentation process could account for slight difference in sugar consumption pattern of the systems. This is contrary to the findings of Rafi *et al.* [36] who observed an increase in itaconic acid production with increase in time of incubation showing maximum yield at day 5. When varying inoculum size, the maximum yield of itaconic acid as shown in Table 3, was observed on day 6 of fermentation with 2 ml having the highest yield and 6ml had the lowest yield on the same day. This could be because lower inoculum size result in lower number of cells in the fermentation medium thereby needing a longer time to grow to the level required to utilize the substrate so as to give desired product [37]. However, there was a decrease in 6 ml which was the highest concentration. This could be due to high spore density thereby leading to rapid consumption of available nutrient leaving limited nutrient for utilization for the production of itaconic acid. This is contrary to the work of Chandragiri and Sastry [38] who observed that maximum production of itaconic acid was obtained with 5 ml of inoculum size of *Ustilago maydis.*

In varying substrate concentration there was a high yield of itaconic acid at day 1 of fermentation for all substrate concentrations with 40g having the highest yield of itaconic acid and the lowest yield was observed on day 4 of fermentation except for substrates concentrations 10g and 15g which had their lowest yield on day 6 of fermentation as shown in Table 4. From the result it was observed that the higher the concentration of the substrate the higher the yield. This result is similar to that of Chandragiri and Sastry [38] who obtained maximum production of itaconic acid on 35% concentration of pure glucose and also concurs with the findings of El Imam *et al*. [30] who obtained maximum production of itaconic acid on 40% concentration of Jatropha Curcas seed cake.

On optimization, *Aspergillus niger* was able to utilize the high substrate concentration 40g and 2 ml inoculums size to produce optimum amount of itaconic acid on day 2 of fermentation as shown in Table 5. This agrees with the findings of El Imam *et al*. [30] who obtained maximum production of itaconic acid on 40% concentration of

Jatropha Curcas seed cake. The substrates acidic level increased at 24 hours interval with day 3 having its acidic level at pH 4.2 as shown in Figure 5. This is also similar to the findings of El Imam *et al*. [30] who obtained the highest yield of itaconic acid at pH 4. pH is one of the most important parameters that affects the production of itaconic acid by fermentation as shown in Figure 1-4 it can be deduced that the highest acidity level throughout the fermentation period was at pH 4.2. This is close to the findings of Rao *et al*. [39] and Chandragiri and Sastry [38] who reported the highest production of itaconic acid at pH 3.5 and 3 respectively and it is also similar to the findings of El Imam *et al*. [30] who obtained the highest yield of itaconic acid at pH 4. From the parameters varied as shown in Table 2-4, it was observed that the substrate being a source of sugar has the ability to produce itaconic acid through fermentation by *Aspergillus niger*. This is in line with the findings of Wilke and Vorlop [5] who observed that itaconic acid is achieved by the fermentation with *Aspergillus niger* on a sugar containing media.

Conclusion

From this study it can be deduced that date fruit, one of the most nutritive fruit is an ideal substrate for the production of organic acids (Itaconic acid) employing solid state fermentation. As observed in the study *Aspergillus niger*, was able to utilize the sugar available in the substrate to produce high quantity of itaconic acid in solid state fermentation. High yield of itaconic acid was shown to depend on the concentration of the substrate, the fermentation period (days) and inoculum size.

Table 1: Proximate Composition of Date Pulp (*Phoenix dactylifera. L*)

Proximate composition	Values (%)
Ash Content	2.00
Moisture Content	6.00
Crude Protein	4.37
Crude Fiber	9.41
Crude Fat	5.93
Soluble Carbohydrate	72.29

Table 2: Effect of Fermentation Period on the production of Itaconic acid from Date pulp (*Phoenix dactylifera. L*) by *Aspergillus niger*

Quantity of Itaconic acid (mg/ml)/ Fermentation Period (days)

Fermentation Period (days)	Values
1	16.88 ± 0.13^{e}
2	15.38 ± 0.38^{d}
3	15.13 ± 0.13^{cd}
4	14.00 ± 0.50^{b}
5	14.25 ± 0.25^{bc}
6	13.50 ± 0.00^{ab}
7	13.75 ± 0.25^{ab}
8	13.13 ± 0.13^{ab}
9	12.75 ± 0.75^{a}
10	13.50 ± 0.00^{ab}

Values represented in the table are means of two replicate readings and standard error of means of Itaconic acid produced in milligram released from milliliter of the substrate as derived from translation of absorbance values using the Itaconic acid standard curve. Values within the column having different superscripts are significantly different at $p<0.05$

Table 3: Effect of Inoculum size on the production of Itaconic acid from Date pulp (*Phoenix dactylifera. L*) by *Aspergillus niger*

Quantity of Itaconic acid (mg/ml)/ Inoculum size (ml)

Inoculum Size(ml)	Days 1	2	3	4	5	6
1	14.25 ± 0.25^{b}	12.75 ± 0.25^{ab}	12.00 ± 0.50^{a}	13.75 ± 0.25^{a}	12.75 ± 0.75^{a}	14.88 ± 0.38^{a}
2	13.00 ± 0.50^{a}	12.00 ± 0.00^{a}	13.25 ± 0.75^{abc}	13.25 ± 0.25^{a}	13.00 ± 0.50^{a}	15.13 ± 1.13^{a}
3	14.50 ± 0.00^{b}	12.75 ± 0.25^{ab}	14.25 ± 0.25^{c}	13.25 ± 0.75^{a}	13.38 ± 0.63^{a}	14.75 ± 0.25^{a}
4	12.75 ± 0.25^{a}	13.00 ± 0.50^{b}	14.00 ± 0.00^{bc}	13.75 ± 0.75^{a}	13.50 ± 1.50^{a}	15.00 ± 0.00^{a}
5	12.75 ± 0.25^{a}	13.00 ± 0.00^{b}	12.75 ± 0.25^{abc}	12.63 ± 0.13^{a}	12.38 ± 0.38^{a}	13.75 ± 0.25^{a}
6	12.50 ± 0.00^{a}	12.75 ± 0.25^{ab}	12.25 ± 0.75^{ab}	12.88 ± 0.13^{a}	12.00 ± 0.00^{a}	13.25 ± 0.25^{a}

Values represented in the table are means of two replicate readings and standard error of means of Itaconic acid produced in milligram released from milliliter of the substrate as derived from translation of absorbance values using the Itaconic acid standard curve. Values within the same column having different superscripts are significantly different at $p<0.05$

Table 4: Effect of Substrate concentration on the production of Itaconic acid from Date pulp (*Phoenix dactylifera. L*) by*Aspergillus niger*

Quantity of Itaconic acid (mg/ml)/ Substrate Concentration (g)

Substrate Conc.(g)	Days 1	2	3	4	5	6
10	19.63±0.63^{a}	17.63±0.13^{a}	16.75±0.25^{a}	15.25±0.00^{c}	16.13±0.13^{ab}	14.63±0.63^{ab}
15	20.50±0.50^{a}	17.00±0.50^{a}	16.25±0.25^{a}	14.75±0.25^{c}	15.63±0.63^{ab}	13.25±0.25^{a}
20	19.13±1.13^{a}	17.50±0.25^{a}	17.38±0.63^{a}	15.25±0.25^{c}	16.00±1.00^{ab}	17.75±0.25^{bc}
25	19.50±0.50^{a}	17.13±0.13^{a}	16.63±0.13^{a}	13.75±0.25^{ab}	15.50±1.00^{ab}	16.00±1.50^{abc}
30	19.00±0.75^{a}	16.88±0.13^{a}	16.63±0.13^{a}	14.00±0.00^{b}	16.50±0.50^{b}	15.63±0.63^{abc}
35	19.00±1.00^{a}	16.75±0.25^{a}	17.13±0.38^{a}	13.25±0.25^{a}	14.00±0.00 ^{a}	14.50±0.00^{ab}
40	20.75±0.25^{a}	18.88±0.13^{b}	17.38±0.63^{a}	14.88±0.13^{c}	15.00±0.00^{ab}	18.50±2.00^{c}

Values represented in the table are means of two replicate readings and standard error of means of Itaconic acid produced in milligram released from milliliter of the substrate as derived from translation of absorbance values using the Itaconic acid standard curve. Values within the same column having different superscripts are significantly different at $p<0.05$

Table 5: Optimum Production of Itaconic Acid from Date Pulp (*Phoenix dactylifera. L*) by *Aspergillus niger*

Quantity of Itaconic acid (mg/ml)
Optimization (days)

Fermentation Days	Quantity of Itaconic acid (mg/ml)
1	19.50±0.50[a]
2	25.00±1.00[b]
3	19.38±1.13[a]

Parameters for optimization are: Date pulp (*Phoenix dactylifera. L*) :- 40g
Fermentation Period:- 3 days Inoculum Size:- 2 ml Temperature:- 28 ^{0}C

Values represented in the table are means of two replicate readings and standard error of means of Itaconic acid produced in milligram released from milliliter of the substrate as derived from translation of absorbance values using the Itaconic acid standard curve. Values within the same column having superscripts are significantly different at $p<0.05$

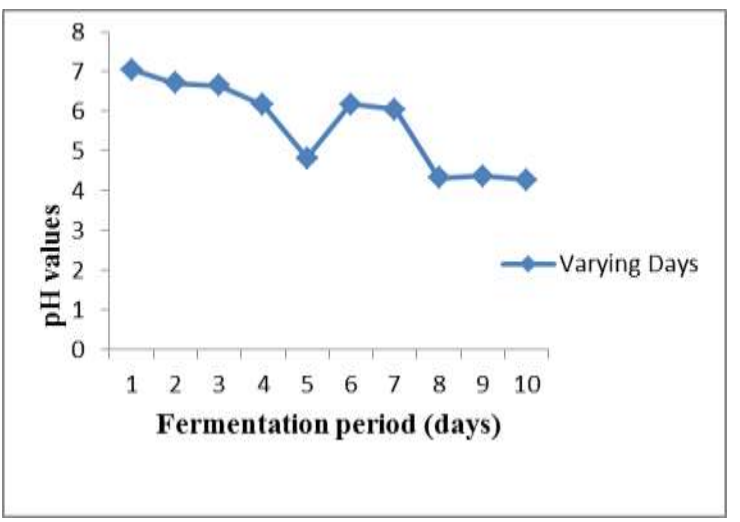

Figure 1: Changes in pH of Date Fruit (Pulp) during different fermentation periods (days) by *Aspergillus niger* for Itaconic acid production

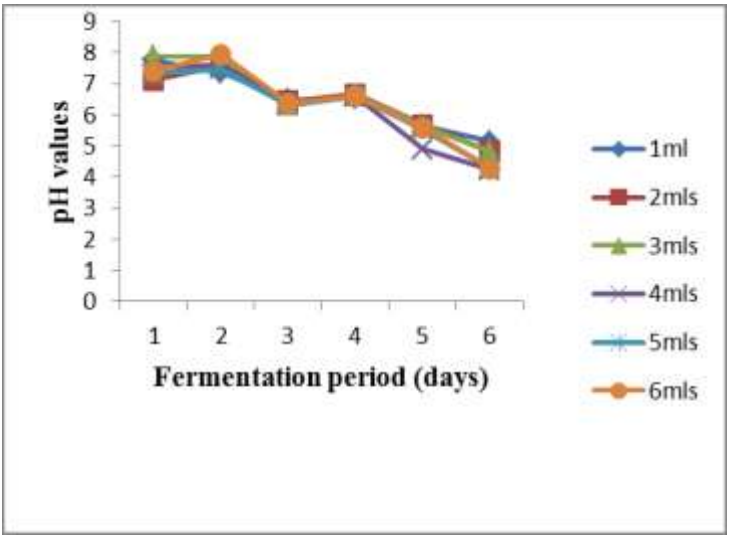

Figure 2: Changes in pH of different inoculums sizes of *Aspergillus niger* during fermentation of Date fruit (pulp) for production of Itaconic acid.

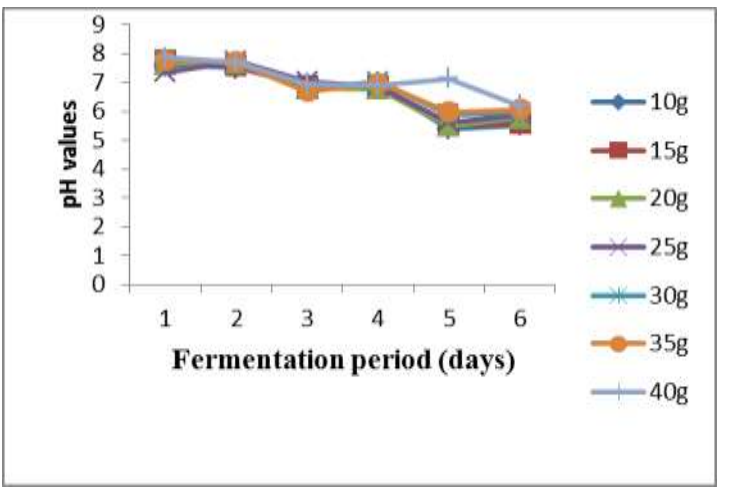

Figure 3: Changes in pH of different concentrations of Date fruit (pulp) during fermentation by *Aspergillus niger* for Itaconic acid production

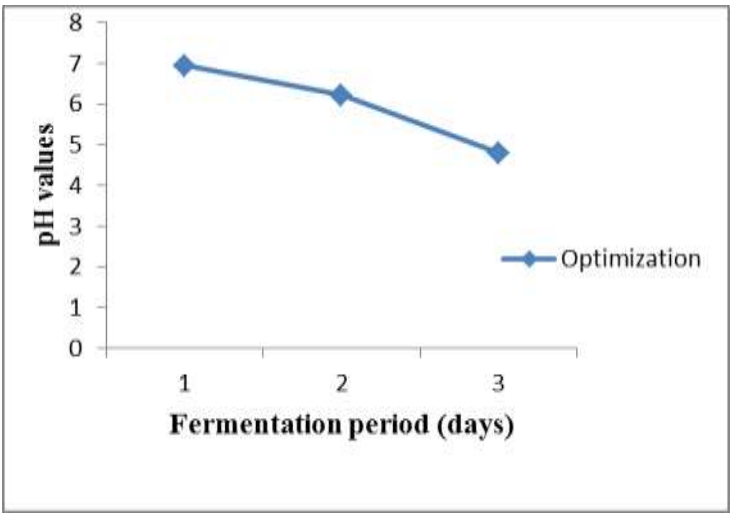

Figure 4: Changes in pH for Optimization of Date fruit (pulp) during fermentation by *Aspergillus niger* for itaconic acid production

References

1 Menon, V. and Rao,M. (2012,) Trends in bioconversion of lignocellulose: Biofuels, platform chemicals and biorefinery concept. Prog. Energ. Combust. 38:522-550.

2 Iqbal, M. and Saeed, A. (2005). *Letters in Applied Microbiology* 40 (3): 178–182.

3 Helia, H. and Wan, M.Y. (2015). Itaconis acid production of microorganism. *Current Journal of Biological Sciences* 7 (2): 37-42.

4 Roehr, M. and Kubicek, C. P. (1996). Further Organic Acids. 2nd Edn., In: Roehr, M. (Ed.), Biotechnology: Products of Primary Metabolism. *VCH VerlagsgesellschaftmbH* 6: 364-379.

5 Willke, T. and Vorlop, K. D. (2001). Biotechnological production of itaconic acid. *Appl. Microbiol. Biotechnol*. 56: 289-295.

6 Menon, V. and Rao, M. (2012). Trends in bioconversion of lignocellulose: Biofuels, platform chemicals and biorefinery concept. *Prog.Energ.Combust.* 38:522-550.

7 Mitsuyasu, O., Dwiarti, L., Shin, K. and Enoch, P. Y. (2009). Biotechnological production of itaconic acid and its biosynthesis in *Aspergillus terreus*. *Appl. Microbiol. Biotechnol*. 84: 597-606.

8 Moshaverinia, A., Roohpour, N., Darr, J. A. and Rehman, I. U. (2009). Synthesis and characterization of a novel N-vinylcarrolactam-containing acrylic acid terpolymer for application in glass-ionomer dental cements. *Acta Biomater*. 5:2101-2108.

9 Culbertson, B.M. (2006). New polymeric materials for use in

glass ionomer cements. *J. Dent*. 4:556-565.

10 Okabe, M., Lies, D., Kanamasa, S. and Park, E. (2009). Biotechnological production of itaconic acid and its biosynthesis in *Aspergillus terreus*. *Appl. Microbiol. Biotechnol*. 84:597-606.

11 Matthias, G., Steiger, M. L., Blumhoff, D.M. and Michael, S. (2013). Biochemistry of microbial itaconic acid production. *Frontier in microbiology*

12 Bentley, R. and Thiessen, C. P. (1957). Biosynthesis of itaconicacidin*Aspergillusterreu s*. III. The propertiesand reaction mechanism of cisaconiticacid decarboxylase. *J. Biol.Chem.* 226: 703–720.

13 Winskill, N. (1983). Tricarboxylic acidcycle activity in relation to itaconicacid biosynthesis by *Aspergillus terreus*. *J. Gen. Microbiol*. 129: 2877–2883.

14 Bonnarme, P., Gillet, B., Sepulchre, A. M., Role, C., Beloeil, J. C. and Ducrocq, C. (1995). Itaconate biosynthesis in *Aspergillus terreus*. *J. Bacteriol*. 177: 3573–3578.

15 Jaklitsch, M., Kubicek, P., Scrutton, C., London, C., Road, C. H. and London, W. (1991). The subcellular organization of itaconate biosynthesis *Aspergillus terreus*. *J. Gen. Microbiol*. 137: 533–539.

16 Strelko, C. L., Lu, W., Dufort, F. J., Seyfried, T. N., Chiles, T. C. and Rabinowitz, J. D. (2011). Itaconic acid is a mammalian metabolitei nduced during macrophage activation. *J. Am. Chem. Soc*. 133:16386–16389.

17 FAOSTAT.http://faostat.fao. org/ DesktopDefault.aspx?PageID= 339&lang=en&country=194 accessed on 23.12.2012. 2010

18 Al-Hooti, S., Sidhu, J. S., Al-Otaibi, J., Al-Ameeri, H. and Qabazard, H. (1997). Processing quality of important date cultivars grown in the United Arab Emirates for jam, butter and dates-in-syrup. *Adv.Food Sci*. 19: 35–40.

19 Lambiote, B. (1982). Some aspects of the role of dates in human nutrition. Proceedings of the First International Symposium on Date palm. King Faisal University, Saudi Arabia, March 23–25.

20 Chandrasekaran, M. and Bahkali, A.H. (2013). Valorization of date palm (*Phoenix dactylifera*) fruit processing by-product and waste using bioprocess technology- *Review*. *Saudi Journal of Biological Sciences* 20: 105-120.

21 Bhargav, S., Panda, B. P., Ali, M. and Javed, S. (2008). Solid-state Fermentation: An Overview. *Chem. Biochem. Eng. Q*. 22 (1):49–70.

2 Kumar, D., Jain, V. K., Shanker, G. and Srivastava, A. (2003). *Process Biochem*. 38: 1731.

23 Lawal, T. E., Iyayi, E. A. and Aderemi, F. A. (2005). Biodegradation of groundnut pod with extracted enzymes from some isolated tropical fungi: growth responses and carcass quality of broilers finisher birds. *Proceedings of*

Annual Conf Animal Sci. Ass. Of Nig. (ASAN). pp. 109-112.

24 Kayode, R. M. O. and Sani, A. (2008). Physicochemical and proximate composition of mango (*Mangifera indica*) kernel cake fermentedwith monoculture of fungal isolates obtained from naturally decomposed mango kernel. *Life Science Journal* 5(4): 55 – 63.

25 Raper, K. B. and Fennell, D. I. (1965). The genus *Aspergillus*. William and Wilkins, Baltimore.

26 Ainsworth, G. C., Sparrow, F. K. and Sussman, A. S. (1973). The fungi – an advanced treatise: A taxonomic review with keys.Ascomycetes and fungi imperfecti, Academic Press, New York, pp. 621.

27 Gilman, J. C. (2001). A manual of soil fungi. Oxford & IBH Publishing Corporation, New Delhi, India.

28 Kuforiji, O. O., Kuboye, A. O. and Odunfa, S. A. (2010). Orange and pineapple wastes as potential substrates for citric acid production. *International Journal of Plant Biology* 1(1): .

29 Fredkin, M. (1945). Determination of itaconic acid in fermentation liquors. *Ind. Eng.Anal.Ed Anal. Ed* 17(10): 637-638.

30 El-Imam, M. A., Kazeem, M. O., Odebisi, M. B., Oke, M. A. and Abidoye, A. O. (2013). Production of itaconic acid from Jatropha curcas seed cake by *Aspergillus terreus*. *Not Sci Biol*. 5(1): 57-61.

31 A.O.A.C. (2000). Official Method of Analysis. 16th Edition. Association of Official Analytical Chemist. Washinton D.C.

32 Xu, D. B., Madrid, C. P., Rohr, M. and Kubicek, C. P. (1989). The influence of type and concentration of the carbon source on production of citric acid by *Aspergillus niger*. *Appl Microbiol Biotechnol*. 30(6):553–558.

33 Amenaghawon, N. A., Areguamen, S. O., Agbroko, N. T., Ogbeide, S. E. and Okieimen, C. O. (2013). Modelling and Statistical Optimisation of Citric Acid Production from Solid State Fermentation of Sugar Cane Bagasse Using *Aspergillus niger*. *International Journal of Sciences Research* Article, 2. http://www.ijSciences.com 2013.

34 Max, B., Salgado, J. M., Rodríguez, N., Cortés, S., Converti, A. and Domínguez, J. M. (2010). Biotechnological production of citric acid. *Braz. J. Microbiol*. 41 (4):

35 Ajiboye, A. E. and Sani, A. (2015). Fermentation of the fruit pulp of *Dialium guineense* for citric acid production using naturally occurring fungi. *International Journal of Current Microbiology and Applied Sciences*. 4(7): 432 – 440.

36 Rafi, M. M., Hanumanthu, M. G., Rao, M. D. and Venkateswarlu, K. (2014). Production of Itaaconic acid by *Ustilago maydis* from agro wastes in solid state fermentation. *J. Biosci. Biotech* 3(2):163-168.

37 Saxena, R. and Singh, R. (2011). Amylase Production by Solid State Fermentation of agro-industrial wastes using *Bacillus* sp. *Braz J Microbial*. 42 (4):1334-1342.

38 Chandragiri, R. and Sastry, R. C. (2011). Synthesis of itaconic acid using *Ustilagomaydis.Canadian J Chem Eng Technol* 2(7):128-135.

39 Rao, D. M., Jaheer, S. M. D., Rangadu, P. V., Subramanyam, K., Sivarama, K. G. and Swamy, A. V. N. (2007). Fermentative production of itaconic acid by *Apergillus terreus* using Jatropha seed cake. *Afr J Biotechnol*. 6(18):2140-2142.

Covenant Journal of Physical & Life Sciences (CJPL) Vol. 6 No. 1, June, 2018

An Open Access Journal available online

Ciprofloxacin Susceptibility Pattern in a Secondary Health Care Facility in Kebbi State, Nigeria

Ajibola, O.,[1]* Aliyu, B.[1] & Usman, K.[2]

[1]Department of Microbiology, Federal University Birnin Kebbi, Kebbi State, Nigeria
[2]Department of Microbiology, Aisha Muhammad Buhari General Hospital, Jega, Kebbi State Nigeria
*olumide.ajibola@fubk.edu.ng, basiru.aliyu@fubk.edu.ng
kabirujamusrumu@gmail.com

***Abstract*:** Antibiotic resistance is a major challenge in management of infectious diseases globally, and particularly in developing countries. There are few studies that have analysed the impact of such abuse on the development of bacterial resistance in Nigeria and sub Saharan Africa. To this end, we retrospectively analysed ciprofloxacin susceptibility patterns in a secondary healthcare facility in Northwest Nigeria over a four year period. Three hundred and thirty six pathogens isolated from 370 patients were analysed in this study. The common pathogens isolated from wound infections were *Staphylococcus aureus* (29, 7.84%), *Pseudomonas* spp (10, 2.7%) and *Proteus* spp (7, 1.89%). In stool samples, *Proteus* (11, 2.97%), *Escherichia coli* (8, 2.2%) and *Salmonella* (6, 1.62%) were the most commonly isolated organisms respectively. While for urine samples, isolates were *S. aureus* (105, 28.37%) followed by *E. coli* from urine samples (62, 16.76%). During the study period, we observed there was a high degree of resistance to ciprofloxacin among *Proteus* spp (50%), *E. coli* (41.3%), *S. aureus* (20.6%), *Klebsiella* (20%) and *Pseudomonas* (20%). Government and stakeholders need to urgently develop antimicrobial stewardship programmes that will address the issue of antibiotic resistance in the country.

Key words: Fluoroquinolones, antibiotic resistance, ciprofloxacin, bacteria, Nigeria

Introduction

The use of antibiotics in clinical practice represents one of the tremendous achievements in the control of infectious diseases. However, the effectiveness of antibiotics has been reduced by an increasing threat of bacterial resistance. Antibiotic resistance (ABR) is the ability of bacteria to survive in antibiotic concentrations that would normally inhibit or kill the bacteria[1]. ABR has emerged as one of the greatest challenges for clinical microbiologists and healthcare practitioners worldwide today[2].Globally, deaths from antibiotic resistant bacteria are estimated to be around 700,000 annually, and projected to rise to 10 million deaths by 2050[3]. Fluoroquinolones are among the most frequently prescribed antimicrobial agents worldwide, since the expiry of the patent on this class of drugs. The European Antimicrobial Resistance Surveillance Network (EARS-Net report, indicates a significant increase in fluoroquinolone resistance across Europe since 2001, with levels ranging from 7% to 53% in 2007[4]. Fluoroquinolones, derivatives of quinolones are stable, orally administrable, broad spectrum agents used to treat a range of bacterial infections. A commonly prescribed fluoroquinolone in developing countries is ciprofloxacin which has broad spectrum activity in treatment of complicated and uncomplicated bacterial infectionsin several anatomical sites, such as respiratory tract infections, otitis media, sinusitis, eye infections, UTI and sepsis [5]. For close to two decades, fluoroquinolones were antibiotics of choice for acute respiratory, enteric and urinary tract infections as well as serious systemic infections such as bacteremia[6]. The frequent prescription of these drugs by healthcare providers, indiscriminate antibiotic use and substandard drugs in developing countries including Nigeria has contributed to the continued spread of ABR to fluoroquinolones[7].

Quinolone resistance in enterobacteria ceae is well documented, and is usually the result of chromosomal mutations leading to alterations in target enzymes or drug accumulation[8]. Single nucleotide polymorphisms in the quinolone resistance determining regions (QRDR) of *gyrA* and *parC*, two of the genes that encode DNA gyrase and topoisomerase IV respectively, can lead to conformational changes in these enzymes that prevents quinolones from binding but still preserve their enzymatic function[9,10]. Mutations in the QRDRs of *gyrA* and *parC* are the most commonly documented quinolone resistance mechanisms, but resistance is also known to be conferred by mutations in the second topoisomerase gene, *pare* [11]. Quinolone resistance can also be acquired horizontally through transferable *aac(6')-Ib* or quinolone resistance (*qnr*) DNA. AAC(6')-Ib encodes a ciprofloxacin acetylating enzyme, while the product of *qnr* inhibits quinolones binding to target proteins [12]. More recently, however, plasmid-mediated quinolone resistance has been reported in *K. pneumoniae* and *E. coli*,

associated with acquisition of the *qnr* gene[8,10,13]. Other ABR mechanisms in bacteria include alteration of cell permeability, site of action of the antibiotic or the release of degrading enzymes[14,15]

In resource poor settings, poor infrastructure, lack of trained laboratory personnel and weak surveillance for ABR contributes to the spread of ABR bacteria. In Nigeria, as with most of SSA there are very few published reports on ABR to fluoroquinolones [6,16], with no published report from Northwest Nigeria. To this end, this study aimed to retrospectively analyseciprofloxacinsusceptibility patterns of commonly isolated bacteria in a secondary health care facility in Kebbi state, Northwest Nigeria.

Materials and Methods

Ethical approval: This study did not carry out any invasive procedures and patients' clinical information was not revealed to the researchers. Ethical approval for use of data was granted by the management of Aisha Muhammadu Buhari General Hospital, Jega, Kebbi State Nigeria.

Setting: Jega local government area (LGA) is one of the twenty-one LGAs in Kebbi state belonging to the Gwandu emirate. Jega LGA has a projected population based on 2006 census of 270,517, comprising mostly muslims, farmers and other low income earners. Jega has only one General hospital (AMBGH) and two private hospitals that provide basic health care services.

Aisha Muhammadu Buhari General Hospital (AMBGH): AMBGHhas an 80 bed capacity and serves a rural population from villages and settlements within Jega LGA. The hospital provides services in diagnosis, curative, promotive and rehabilitative services in medical treatment and an outpatient clinic. AMBGH is staffed by one physician supported by fifteen nurses and midwives, and a microbiology laboratory led by a qualified laboratory scientist. The facility has minimal laboratory facilitiesand can only carry out urine, stool, sputum culture, microscopy, biochemical, immunological tests, HIV screening and tuberculosis testing.

Sample collection: This was a retrospective study of the data on fluoroquinolone resistance patterns carried out in Jega local government area (LGA), Kebbi state, Northwest Nigeria, at the department of microbiology of (AMBGH), Jega, Kebbi State Nigeria. All microbiology reports for urine, stool, vaginal swabs and wound samples between June 2014 and September 2017 were included for analysis. For this study, we excluded data with incomplete sensitivity results, and all samples for microbiological analysis were referred to the laboratory by the physician.

Microbiological analyses: Patients referred to the microbiology laboratory by the physician were provided with labelled specimen bottles and trained on how and when to provide samples for laboratory diagnosis. All samples brought to the laboratory were immediately processed following standard bacteria culture procedures. Biochemical characterization of isolates was carried out under the strict supervision of a medical laboratory scientist licensed by the Medical and Laboratory Science Council of Nigeria (MLSCN). Antibiotic susceptibility

testing was carried out following the Clinical Laboratory Standards Institute (CLSI) guidelines [27]. In this study, we report the rates of susceptibility and resistant isolates. AMBGH microbiology laboratory is regularly subjected to external audits by the MLSCN to assess the state of the facility for providing routine diagnostic services.

Statistics: Data were accumulated and analysed with Microsoft excel and Stata version 12 software (College Station, Texas, USA) to generate differential descriptive statistics including frequency tables thatshowed the frequency and percentage distribution of isolates.

Results

Demographics

In total three hundred and seventy patients were sampled at the microbiology laboratory of AMBGH between June 2014 and September 2017. For the study period reviewed, the ratio of male to female sampled was 0.47:1.0, and the median age of the children was 10 yrs (IQR, 15 yrs) and that of adults was 35 yrs (IQR, 21 yrs) respectively (Table 1).

Bacteria spectrum

In total 336 isolates were included within the study period reviewed. There were no significant differences (P=0.09) in the isolates collected among children or adults (Table 2). The most frequent isolate was *Staphylococcus aureus* from urine samples (105, 28.37%) followed by *Escherichia coli* from urine samples (62, 16.76%). From wound infections the most frequent isolate was *S. aureus* (29, 7.84%), followed by *Pseudomonas* spp (10, 2.7%) and *Proteus* spp (7, 1.89%). In stool samples, *Proteus* (11, 2.97%), *E. coli* (8, 2.2%) and *Salmonella* (6, 1.62%) were the most commonly isolated organisms respectively (Table 3). Other samples such as sputum and high vaginal swabs revealed *S. aureus* to be the main pathogenic organism isolated in culture.

Antibiotic susceptibility

Next we assessed the proportion of isolates that were not susceptible to ciprofloxacin from antibiotic sensitivity tests carried out using the disk diffusion method. During the study period, we observed there was a high degree of resistance to ciprofloxacin among *Proteus*spp (50%), *E. coli* (41.3%), *S. aureus* (20.6%), *Klebsiella* (20%) and *Pseudomonas* (20%) respectively. Susceptibility to ciprofloxacin by the isolates was highest in *Salmonella* (71.4%), *S. aureus* (65.2%), *Klebsiella* (60%), *Pseudomonas* (60%), *E. coli* (41.3%), and *Proteus* (40%) respectively. Other isolates within the study period reviewed demonstrated intermediate level susceptibility (Table 4).

Discussion

In developing countries, antibiotics use without prescription due to their availability over the counter appears to be the norm, in addition to sub-optimal health care systems that lack the capacity to provide timely laboratory results for clinicians to make decisions with. These issues and others promote the rapid increase in the spread of antibiotics resistant bacteria in resource poor settings. Here we review four year microbiological data from a secondary health care facility in a rural area in Northwest Nigeria. This was carried out in order to provide valuable laboratory information for clinicians

and health care practitioners on the pattern of ciprofloxacin susceptibility, in the absence of routine antibiotic resistance surveillance activities. Our data suggests that the most commonly isolated pathogen from samples and swabs analysed was *S. aureus*, followed by *E. coli*. Our findings also revealed a high degree of ciprofloxacin resistance in the isolates, with *Proteus* spp demonstrating most resistance (50%), followed by *E. coli*(41.3%). In a five year retrospective study carried out in Bahia, Brazil a high degree of ciprofloxacin resistance was observed in community acquired urinary tract infection isolates from the participants. Ciprofloxacin resistance was highest in *E. coli* isolates, with up to 36% of the isolates in a particular year being resistant[17]. In a retrospective study in Gabon, ciprofloxacin resistance of 24.1% was also reported in *E. coli*[18]. Quinolone resistance has also been reported in Cameroon from S. Typhi and Ghana in*Vibrio cholerae* respectively [19,20]. Studies on fluoroquinolones resistance in Africa, including Nigeria are very scarce. The few published papers on fluoroquinolones resistance in Nigeria clearly suggest the circulation of ciprofloxacin resistant bacteria in the country[16,21–25]. In a study carried out in Minna, north central Nigeria, the authors found that *Salmonella enterica* serovar Typhi were resistant to commonly prescribed antibiotics ceftriaxone, cefuroxime, amoxicillin, ampicillin, ciprofloxacin, and augmentin[26]. The increase in treatment failures to β-lactams and sulfamethoxazole+trimethoprim over the past years led to the use of fluoroquinolones as the first choice, hence putting pressure on the use of this drug as first line therapy for most bacterial infections.

The review of microbiological data from the secondary health care facility in this study reveals an alarming trend of ciprofloxacin resistance in the population. Our study also provides local ABR data which could be used by clinicians in the region to guide clinical decisions. Ciprofloxacin, a broad spectrum antibiotic is widely used in management of infections in developing countries. Our study suggests the need to establish surveillance for ABR in Nigeria and Africa in general, replicating the approach of the European Antimicrobial Resistance Surveillance Network (http://ecdc.europa.eu/en/activities/surveillance/ EARS-Net/Pages/index.aspx), which monitors antibiotic consumption in comparison to spread of resistance. In developing countries, the challenge of managing the spread of ABR is enormous, owing to lack of good sanitation practices, lack of potable water, poor hygiene, high poverty levels, illiteracy and sub-optimal healthcare systems. Hence, there is a need for African governments to have short term goals that will produce significant results in dealing with the menace of ABR.

This study has some limitations, first is the inability of the health facility considered in this study to carry out blood culture to isolate pathogens in the blood of patients. Lack of blood culture facility is one of the major challenges facing diagnostic laboratories in Africa, and even when present, the approach used might be sub-optimal or lack the required sensitivity. Inability to carry out blood culture in this facility has potentially

excluded bacteria that might be important in our understanding of the ciprofloxacin resistant bacteria circulating in the population. Second, incessant power cut offs also made it impossible for the facility to preserve multidrug resistant isolates for molecular studies. Hence the underlying molecular mechanisms of resistance in the isolates are unclear. Third, the isolates described here do not distinguish between community or hospital acquired infections based on the records made available by the health facility. Lastly, it is possible that the number of isolates reported in this study might be below the true number of isolates actually reported due to poor record keeping which is common to most African hospitals, but that might not be the case in our study.

To conclude, it is very likely that fluoroquinolones resistance emerged with increase in their indiscriminate use [6], hence there is an urgent need for establishing an antimicrobial stewardship programme that will address antibiotic use in humans and animals. This programme should be designed to complement improving the quality of laboratories, and establishing a national surveillance programme to detect, report and monitor multidrug resistant bacteria strains.

Acknowledgements

We thank the management of AMBGH for approving the use of the data for this retrospective study.

References

1. Alós, J.-I. [Antibiotic resistance: A global crisis]. Enferm. Infecc. Microbiol. Clin.2015, 33, 692–699, doi:10.1016/j.eimc.2014.10.004.
2.Jung, C. M. Dissemination of Bacterial Fluoroquinolone Resistance in Two Multidrug-Resistant Enterobacteriaceae. J. Mol. Microbiol. Biotechnol.2014, 24, 130–134, doi:10.1159/000362278.
3.Williams, D. N. Antimicrobial resistance: are we at the dawn of the post-antibiotic era? J. R. Coll. Physicians Edinb.2016, 46, 150–156, doi:10.4997/JRCPE.2016.302.
4. Paltansing, S.; Kraakman, M. E. M.; Ras, J. M. C.; Wessels, E.; Bernards, A. T. Characterization of fluoroquinolone and cephalosporin resistance mechanisms in Enterobacteriaceae isolated in a Dutch teaching hospital reveals the presence of an Escherichia coli ST131 clone with a specific mutation in parE. J. Antimicrob. Chemother.2013, 68, 40–45, doi:10.1093/jac/dks365.
5. Andriole, V. T. The quinolones: past, present, and future. Clin. Infect. Dis. Off. Publ. Infect. Dis. Soc. Am.2005, 41 Suppl 2, S113-119, doi:10.1086/428051.
6. Lamikanra, A.; Crowe, J. L.; Lijek, R. S.; Odetoyin, B. W.; Wain, J.; Aboderin, A. O.; Okeke, I. N. Rapid evolution of fluoroquinolone-resistant Escherichia coli in Nigeria is temporally associated with fluoroquinolone use. BMC Infect. Dis.2011, 11, 312, doi:10.1186/1471-2334-11-312.
7. Tytler, B. A.; Mijinyawa, N.; Ida, A. Comparative quality of fluoroquinolone tablets marketed in some towns in Northern

Nigeria. J Pharm Bioresources2007, 4, 8–13.

8.Tran, J. H.; Jacoby, G. A. Mechanism of plasmid-mediated quinolone resistance. Proc. Natl. Acad. Sci. U. S. A.2002, 99, 5638–5642, doi:10.1073/pnas.082092899.

9.Karczmarczyk, M.; Martins, M.; Quinn, T.; Leonard, N.; Fanning, S. Mechanisms of Fluoroquinolone Resistance in Escherichia coli Isolates from Food-Producing Animals. Appl. Environ. Microbiol.2011, 77, 7113–7120, doi:10.1128/AEM.00600-11.

10.Blair, J. M. A.; Webber, M. A.; Baylay, A. J.; Ogbolu, D. O.; Piddock, L. J. V. Molecular mechanisms of antibiotic resistance. Nat. Rev. Microbiol.2015, 13, 42–51, doi:10.1038/nrmicro3380.

11.Hopkins, K. L.; Davies, R. H.; Threlfall, E. J. Mechanisms of quinolone resistance in Escherichia coli and Salmonella: recent developments. Int. J. Antimicrob. Agents2005, 25, 358–373, doi:10.1016/j.ijantimicag.2005.02.006.

12.Tran, J. H.; Jacoby, G. A. Mechanism of plasmid-mediated quinolone resistance. Proc. Natl. Acad. Sci. U. S. A.2002, 99, 5638–5642, doi:10.1073/pnas.082092899.

13.Redgrave, L. S.; Sutton, S. B.; Webber, M. A.; Piddock, L. J. V. Fluoroquinolone resistance: mechanisms, impact on bacteria, and role in evolutionary success. Trends Microbiol.2014, 22, 438–445, doi:10.1016/j.tim.2014.04.007.

14.Wright, G. D. Bacterial resistance to antibiotics: enzymatic degradation and modification. Adv. Drug Deliv. Rev.2005, 57, 1451–1470, doi:10.1016/j.addr.2005.04.002.

15.Machuca, J.; Briales, A.; Díaz-de-Alba, P.; Martínez-Martínez, L.; Pascual, Á.; Rodríguez-Martínez, J.-M. Effect of the efflux pump QepA2 combined with chromosomally mediated mechanisms on quinolone resistance and bacterial fitness in Escherichia coli. J. Antimicrob. Chemother.2015, 70, 2524–2527, doi:10.1093/jac/dkv144.

16.Aibinu, I.; Aednipekun, E.; Odugbemi, T. Emergence of Quinolone Resistance amongst Escherichia coli strains isolated from Clinical infections in some Lagos State Hospitals, in Nigeria. Niger. J. Health Biomed. Sci.2004, 3, doi:10.4314/njhbs.v3i2.11513.

17. REIS, A. C. C.; SANTOS, S. R. da S.; de SOUZA, S. C.; SALDANHA, M. G.; PITANGA, T. N.; OLIVEIRA, R. R. CIPROFLOXACIN RESISTANCE PATTERN AMONG BACTERIA ISOLATED FROM PATIENTS WITH COMMUNITY-ACQUIRED URINARY TRACT INFECTION. Rev. Inst. Med. Trop. São Paulo2016, 58, doi:10.1590/S1678-9946201658053.

18.Alabi, A. S.; Frielinghaus, L.; Kaba, H.; Kösters, K.; Huson, M. A. M.; Kahl, B. C.; Peters, G.; Grobusch, M. P.; Issifou, S.;

Kremsner, P. G.; Schaumburg, F. Retrospective analysis of antimicrobial resistance and bacterial spectrum of infection in Gabon, Central Africa. BMC Infect. Dis.2013, 13, 455, doi:10.1186/1471-2334-13-455.

19.Nkemngu N, M. Susceptibility patterns of Salmonella enterica serovar Typhi to 10 antibiotics in Cameroon. In; Guilin, China; Vol. 99.

20.Opintan, J. A.; Newman, M. J.; Nsiah-Poodoh, O. A.; Okeke, I. N. Vibrio cholerae O1 from Accra, Ghana carrying a class 2 integron and the SXT element. J. Antimicrob. Chemother.2008, 62, 929–933, doi:10.1093/jac/dkn334.

21.Fortini, D.; Fashae, K.; Villa, L.; Feudi, C.; García-Fernández, A.; Carattoli, A. A novel plasmid carrying blaCTX-M-15 identified in commensal Escherichia coli from healthy pregnant women in Ibadan, Nigeria. J. Glob. Antimicrob. Resist.2015, 3, 9–12, doi:10.1016/j.jgar.2014.12.002.

22.Fashae, K.; Hendriksen, R. S. Diversity and antimicrobial susceptibility of Salmonella enterica serovars isolated from pig farms in Ibadan, Nigeria. Folia Microbiol. (Praha)2014, 59, 69–77, doi:10.1007/s12223-013-0270-6.

23.Aibinu, I.; Pfeifer, Y.; Peters, F.; Ogunsola, F.; Adenipekun, E.; Odugbemi, T.; Koenig, W. Emergence of bla(CTX-M-15), qnrB1 and aac(6')-Ib-cr resistance genes in Pantoea agglomerans and Enterobacter cloacae from Nigeria (sub-Saharan Africa). J. Med. Microbiol.2012, 61, 165–167, doi:10.1099/jmm.0.035238-0.

24.Akinyemi, K. O.; Bamiro, B. S.; Coker, A. O. Salmonellosis in Lagos, Nigeria: Incidence of Plasmodium falciparum-associated Co-infection, Patterns of Antimicrobial Resistance, and Emergence of Reduced Susceptibility to Fluoroquinolones. J. Health Popul. Nutr.2007, 25, 351–358.

25.Aibinu, I.; Odugbemi, T.; Koenig, W.; Ghebremedhin, B. Sequence type ST131 and ST10 complex (ST617) predominant among CTX-M-15-producing Escherichia coli isolates from Nigeria. Clin. Microbiol. Infect. Off. Publ. Eur. Soc. Clin. Microbiol. Infect. Dis.2012, 18, E49-51, doi:10.1111/j.1469-0691.2011.03730.x.

26.Adabara, N. U.; Ezugwu, B. U.; Momojimoh, A.; Madzu, A.; Hashiimu, Z.; Damisa, D. The Prevalence and Antibiotic Susceptibility Pattern of Salmonella typhi among Patients Attending a Military Hospital in Minna, Nigeria Available online: https://www.hindawi.com/journals/apm/2012/875419/ (accessed on Mar 21, 2018).

27.CLSI Standards Center: Our Standards Help Foster Health Care Excellence Available online: https://clsi.org/standards/ (accessed on Nov 13, 2017).

Table 1. Demographics of patients

	Children (≤ 18 yrs)	Adult (> 18 yrs)
	54	316
Median age (IQR)	10	35
	Male	Female
Sex, n (%)	119 (32.2%)	251 (67.8%)

Table 2. Distribution of isolates from children and adults

Isolates	*Proteus spp*	*Klebsiella*	*Pseudomonas*	*Staphylococcus aureus*	*Escherichia coli*	*Salmonella*
Children (≤18 yrs)	7	-	3	28	14	2
Adults (>18 yrs)	23	10	7	176	61	5
Total	30	10	10	204	75	7

Table 3. Source of isolates from patients' samples

Samples	*Proteus spp*	*Klebsiella*	*Pseudomonas*	*Staphylococcus*	*Escherichia coli*	*Salmonella*
Wound infections	7	3	10	29	-	-
Urine infections	21	7	-	105	62	1
High vaginal swab	-	-	-	20	4	-
Sputum	-	-	-	50	1	-
Stool	11	-	-	-	8	6
Total	30	10	10	204	75	7

Table 4. Susceptibility pattern of bacterial isolates to ciprofloxacin

Samples	*Proteus spp*	*Klebsiella*	*Pseudomonas*	*Staphylococcus*	*Escherichia coli*	*Salmonella*
Susceptible	12 (40%)	6 (60%)	6 (60%)	133 (65.2)	31 (41.3%)	5 (71.4%)
Intermediate	3 (10%)	2 (20%)	2 (20%)	29 (14.2%)	13 (17.4%)	1 (14.3%)
Resistant	15 (50%)	2 (20%)	2 (20%)	42 (20.6%)	31 (41.3%)	1 (14.3%)
Total	30 (100%)	10 (100%)	10 (100%)	204 (100%)	75 (100%)	7 (100%)

Covenant Journal of Physical & Life Sciences (CJPL) Vol. 6 No. 1, June, 2018

An Open Access Journal available online

A Mathematical Model on Cholera Dynamics with Prevention and Control

Ayoade A. A. [1], Ibrahim M. O. [1], Peter O. J., [1]*& Oguntolu F. A.[2]

[1]Department of Mathematics, University of Ilorin, Nigeria
[2]Department of Mathematics/Statistics,
Federal University of Technology, Minna, Nigeria
* peterjames4real@gmail.com

Abstract: In this paper, we present and analyze a cholera epidemiological model with modifications to Fung (2014) cholera model. The extended model incorporates preventive and control measures as well as the possibility of disease transmission from person-to-person. Equilibrium analysis is conducted for the extended model for two cases of epidemic equilibrium and endemic equilibrium to establish disease free equilibrium state (DFE) and endemic equilibrium state (EE) respectively. We derive the basic reproduction numbers and establish the local asymptotical stability for the two models. We later use the results to compare the models at the DFE states as regards the effects of control on the extended model. The endemic equilibrium state (EE) of the extended model is also studied and found to be locally asymptotically stable when the basic reproduction number . This shows that cholera can be eliminated in a population only if the preventive and control measures are strong enough.

Keywords: model, equilibrium, reproduction number, stability

Introduction

Cholera is an acute intestinal water-borne infectious disease. It is a potentially epidemic and life-threatening secretory diarrhea that is caused by the bacterium Vibrio Cholerae, first identified by Robert Koch in 1883 during a cholera outbreak in Egypt and characterized by numerous, voluminous watery stools, often accompanied by vomiting and resulting in hypovolenic shock and acidosis (Finkelstein, 2013). Though cholera is preventable and curable, the

current global cholera report indicates that there are an estimated 3 – 5 million cholera cases and 100 000 – 120 000 deaths due to cholera every year [1].

The complexity of cholera dynamics stems from the fact that both direct (i.e. human-to –human) and indirect (i.e. environment-to-human) routes are involved in the disease transmission [2]. The environment-to-human way of transmitting cholera is mainly through ingesting Vibrio Cholerae bacteria from contaminated food or water while human-to-human way of cholera transmission is mostly unhygienic contact with cholera patient'sfaeces, vomit or corpse [3]. Although cholera is well prevented in developed countries of the world, recent data show that the global outbreak of cholera is rising in Africa and the entire less developed countries. This rise may be attributed to inadequate access to safe drinking water supply, improper treatment of reservoirs and improper sanitation [4].

While cholera has been a recognized disease for more than a century, its occurrence in developing countries including Nigeria has been alarming and has become a subject of concern. In 1971, 22,931 cases of cholera and 2,945 deaths with a case fatality rate (CFR) of 12.8% were recorded in Nigeria. The disease reoccurred in 1991 in which 59,478 cases and 7,654 deaths were reported. The CFR was 12.9% which remains the highest rate reported by the country to date. Also, in 2009, Nigeria reported 13,691 cases and 431 deaths [5]. Furthermore, in 2005, Nigeria had 4,477 cases and 174 deaths and in 2008, there were reported cases of 6,330 and 429 deaths [6].

Several mathematical models have been proposed to understand the transmission dynamics and control of cholera [3, 6]In all of these models, the use of vaccination and antibiotics to control cholera are played down. Nevertheless, the place of vaccination and antibiotics in fighting against the propagation of infectious diseases cannot be underestimated. Vaccination reduces the number of fully susceptible individuals, reduces infectiousness (i.e the rate of contamination of the water supply), and reduces the probability of becoming symptomatic when infected. Also, antibiotics administration shortens the duration of illness and perhaps reduces the concentration of Vibrios excreted during illness [7].

Chao et al. (2011) claimed that the use of vaccines would likely have minimized the calamity that befell Haiti in 2010 in terms of reduction in morbidity and mortality of cholera, but such vaccines were in short supply and little was known about effective vaccination strategies for epidemic cholera. The researchers also examined prevaccination strategies in which vaccination occurs well before the epidemic starts and reactive vaccination strategies in which vaccination begins after the epidemic has started and discovered that randomly prevaccinating a fraction of the population well before the epidemic begins can reduce the number of cases roughly in proportion to the number of individuals vaccinated and delay the epidemic peak.

Benefits from an intervention are a combination of direct effects on those receiving the intervention and indirect effects on those with reduced exposure

because others received the intervention. In the context of vaccination, producing immunity through vaccination of only a part of the population may stop an epidemic because chains of transmission are broken – a concept known as "herd protection"[7]. Concentration of prevaccination in areas at high risk of cholera, such as along rivers and other bodies of fresh water can help achieve critical vaccination threshold – the proportion of the population one would need to vaccinate effectively to stop an epidemic [8]. The cholera vaccines are safe, effective and have an efficacy against clinical disease of over 65% lasting at least 3 – 5 years [9]

The study conducted by the research arm of the international medical humanitarian organization [10] and the Guinean Ministry of Health revealed that an oral cholera vaccine (i.e. Shanchol) protected individuals by 86% during the 2012 cholera outbreak in Guinea (MSF, 2012). Since most existing cholera models exclude the use of vaccination and antibiotics as measures against cholera despite their roles in fighting against the propagation of infectious diseases, this work is aimed to better understand the effects of these measures so as to gain useful guidelines to the effective prevention and intervention strategies against cholera epidemics. To that end, we study cholera dynamics with prevention and control measures as well as the possibility of disease transmission from person-to-person incorporated into the model of [11] which involve only the environment-to-human transmission mode

Material and Methods

Formulation of model

Let S(t), I(t) and R(t) represent the susceptible, the infected, and the recovered human populations, respectively. The total human population N = S + I + R is closed, which is a reasonable assumption for a relatively short period of time and for low – mortality diseases like cholera. For example, WHO states that "In 2012, the overall case fatality rate for cholera was 1.2 %"[12] Also, let B denote the concentration of the Vibrios in the environment (i.e. contaminated water). The following assumptions are made to extend [11] cholera model:

(i) Vaccination is introduced to the susceptible population at a rate v1(t), so that v1(t)S(t) individuals per time are removed from the susceptible category and added to the recovered population.

(ii)Therapeutic treatment and vaccination are applied to the infected people at a rate

(t), and v2(t) respectively so that (t)I(t) and v2(t)I(t) individuals per time are removed from the infected class and added to the recovered class. Therapeutic treatment is in the form of administration of antibiotics or rehydration salts. As a result of modifications, the new model equations are as follows:

$$\left.\begin{aligned}
\frac{dS}{dt} &= \pi - \mu S - \varphi S - \gamma_1 S + \sigma R \\
\frac{dI}{dt} &= \varphi S - (\mu + \mu_c + \gamma_2 + \rho + \gamma) I \\
\frac{dR}{dt} &= \gamma I - \mu R + \gamma_2 I + \gamma_1 S + \rho I - \sigma R \\
\frac{dB}{dt} &= \varepsilon I - \delta B
\end{aligned}\right\} \quad (1)$$

$$\varphi = \left[\frac{\beta_1 B}{(B+\aleph)} + \beta_2 I\right] \quad (2)$$

Where
$S(0) > 0, B(0) \geq 0, I(0) \geq 0, R(0) \geq 0.$
All the parameters are non-negative and $\beta_1 > \beta_2$.
π is the recruitment rate of susceptible individuals, γ is the natural recovery rate , μ and μ_c are death rates, unrelated to cholera and due to cholera respectively, σ is the rate of losing immunity, φ is the force of infection, v_1 and v_2 are vaccination rates, before and after the outbreak respectively, ρ is the rate of applying therapeutic treatment, ε is the rate at which infectious individuals contribute V. cholerae to the water reservoir, δ is the death rate of V. cholerae unrelated to water treatment, $\aleph$ is the concentration of V. cholerae in the water reservoir that will make 50% of the susceptible population ill and β_1 and β_2 represent rates of ingesting Vibrios from the contaminated water and through human – to – human interaction, respectively

Equilibrium analysis

For the special case when the rates of prevention and control are positive constants,
i.e v(t) = $v_1 > 0$, $v_2 > 0$ and $\rho(t) = \rho > 0$, the model eqn. (1) using eqn. (2) is reduced to an autonomous system

$$\frac{dS}{dt} = \pi - \mu S - \frac{\beta_1 B}{B+\aleph} S - \beta_2 IS - v_1 S + \sigma R \quad (3)$$

$$\frac{dI}{dt} = \frac{\beta_1 B}{B+\aleph} S + \beta_2 IS - (\mu + \mu_c + v_2 + \rho + \gamma) I \quad (4)$$

$$\frac{dB}{dt} = \varepsilon I - \delta B \quad (5)$$

$$\frac{dR}{dt} = \gamma I - \mu R + v_2 I + v_1 S + \rho I - \sigma R \quad (6)$$

Permanent immunity is assumed therefore, equation (6) is not needed in the model analysis. This is done for convenience of discussion [12,13]. Besides in (3) is dropped since compartment R is not included in the analysis.
This allows us to conduct a careful equilibrium analysis to investigate the effects of protection and control on the epidemic and endemic dynamics of cholera.

Epidemic Dynamics

The disease-free equilibrium (DFE) for the model is given by

$$E_0 = \left(\frac{\pi}{\mu+v_1}, 0, 0\right). \quad (7)$$

Having determined the disease free equilibrium point E_0, we proceeded to compute the basic reproduction number for the two models using the method of [14]. The associated next generation matrices are given by

$$F = \begin{pmatrix} \beta_2 S & \frac{\beta_1 S}{B+\aleph} - \frac{\beta_1 BS}{(B+\aleph)^2} \\ 0 & 0 \end{pmatrix}, V = \begin{pmatrix} (\mu+\mu_c+v_2+\rho+\gamma) & 0 \\ -\varepsilon\delta & \end{pmatrix} \quad (8)$$

The basic reproduction number is then determined as the spectral radius of FV^{-1}, which yields

$$R_0{}^q = \rho(FV^{-1}) = \frac{\pi\varepsilon\beta_1 + \pi\aleph\delta\beta_2}{\aleph\delta(\mu+v_1)(\mu+\mu_c+v_2+\rho+\gamma)} \quad (9)$$

The superscript q is used to emphasize the model with controls. Compared to the basic reproduction number for the original no-control model (Fung, 2014) which is given as

$$R_0 = \frac{\mu_b\beta N}{\aleph\mu_d(\gamma+\mu_c+\mu_d)} \quad (10)$$

Clearly, $R_0{}^q \leq R_0$ and the result in (9) shows that, mathematically, each of the controls can reduce the value of $R_0{}^q$ below 1 so that the disease will be eradicated though the combination of the two interventions would achieve better result.

It follows from theorem 2 in [15] that the disease- free equilibrium is locally asymptotically stable when $R_0{}^q < 1$. In contrast, if the controls are weak such that $R_0{}^q > 1$, then the disease-free equilibrium is unstable and a disease outbreak occurs.

Local Stability of the Disease Free Equilibrium (DFE)

If the controls are assumed to be weak and an outbreak occurs then there is a need to compare the outbreak growth rates between the original no - control model and the model with controls. We shall use the linearization approach to analyze the effect of weak prevention and control measures on the extended model. The positive (dominant) eigenvalue of the Jacobian matrix at the DFE characterizes the initial outbreak growth rate [16].

For the system of equations (3) – (5), the Jacobian matrix at the DFE is given by

$$J(E_0) = \begin{bmatrix} \frac{-\beta_1 S}{B+\aleph} - \beta_2 I - \mu - v_1 & -\beta_2 S & -\frac{\beta_1 S}{B+\aleph} + \frac{\beta_1 BS}{(B+\aleph)^2} \\ \frac{\beta_1 B}{B+\aleph} + \beta_2 I & \beta_2 S - (\mu+\mu_c+v_2+\rho+\gamma) & \frac{\beta_1 S}{B+\aleph} - \frac{\beta_1 BS}{(B+\aleph)^2} \\ 0 & \varepsilon & -\delta \end{bmatrix} \quad (11)$$

At the disease free equilibrium state, using the expression E_0 i.e put eqn. (7) in eqn. (11), we obtain

$$J(E_0) = \begin{bmatrix} -\mu - v_1 & \frac{-\pi\beta_2}{(\mu+v_1)} & \frac{-\pi\beta_1}{\aleph(\mu+v_1)} \\ 0 & \frac{\pi\beta_2}{(\mu+v_1)} - (\mu+\mu_c+v_2+\rho+\gamma) & \frac{\pi\beta_1}{\aleph(\mu+v_1)} \\ 0 & \varepsilon & -\delta \end{bmatrix} \quad (12)$$

The characteristic equation in λ is obtained from the Jacobian determinant thus,

$$(\mu + v_1 + \lambda)\left[\lambda^2 + (\mu+\mu_c+v_1+\rho+\gamma+\delta-\beta_2 S_0)\lambda + \delta(\mu+\mu_c+v_2+\rho+\gamma) - \left(\frac{\varepsilon\beta_1}{\aleph} + \delta\beta_2\right)S_0\right] = 0, \quad (13)$$

where $S_0 = \frac{\pi}{(\mu+v_1)}$.

The necessary and sufficient conditions for the DFE of the model to be locally asymptotically stable is for all the eigenvalues of eqn. (13) to be negative

Clearly the first eigenvalue is:

$$\lambda_1 = -(\mu + v_1)$$

The remaining part of the characteristic equation is given as:

$$\left[\lambda^2 + (\mu+\mu_c+v_1+\rho+\gamma+\delta-\beta_2 S_0)\lambda + \delta(\mu+\mu_c+v_1+\rho+\gamma) - \left(\frac{\varepsilon\beta_1}{\aleph} + \delta\beta_2\right)S_0\right] = 0$$

In the absence of the disease (i.e. DFE), there is no transmission of infection either from person-to-person or from water-to-person which makes β_1 andβ_2 to be zero in the above equation hence, all the eigenvalues in eqn. (13) are negative and the DFE of the extended model is locally asymptotically stable for$R_0{}^q < 1$.

As speculate earlier, suppose the controls are weak and there is an outbreak i.e$\beta_1 \neq 0$ and $\beta_2 \neq 0$ such that $R_0{}^q > 1$ then there will be at least one positive eigenvalue for eqn. (13). Let $\lambda_+{}^q$ denote the eigenvalue and it exists if and only if $\delta(\mu + \mu_c + v_2 + \rho + \gamma) <$ $\left(\frac{\varepsilon\beta_1}{\aleph} + \delta\beta_2\right) S_0$. This is the sufficient condition for the product of the remaining roots of eqn. (13) to be negative.

In terms of graph, the value of $\lambda_+{}^q$ is the slope of the ascending infection curve when $R_0{}^q > 1$ and the higher the$\lambda_+{}^q$ the higher the severity of disease outbreak. Obviously, $\lambda_+{}^q > 0$ when $R_0{}^q > 1$ and$\lambda_+{}^q < 0$ when $R_0{}^q < 1$. This result can be interpreted by the values of the controls. The disease easily breaks out and easily sustained if $v_1 = v_2 = \rho = 0$ whereas the initial disease outbreak growth rate is prevented or eradicated if the strength of v_1, v_2 and ρ is strong enough.

For the purpose of comparison, the quadratic part of the characteristic equation of the original no-control cholera model for $R_0 > 1$ is evaluated in a similar way as in eqn. (13) and it is given as

$$\left[\lambda^2 + (\mu_d + \mu_c + \gamma + \delta)\lambda + \delta(\mu_d + \mu_c + \gamma) - \left(\frac{\varepsilon\beta}{\aleph}\right)S_0\right] = 0, \quad (14)$$

where $S_0 = \frac{\mu_b N}{\mu_d}$. If λ_+ is the positive eigenvalue of the original no-control cholera model then, $\lambda_+{}^q \leq \lambda_+$ if $v_1 \geq 0,\ v_2 \geq 0$ and $\rho \geq 0$ while $\lambda_+{}^q \geq \lambda_+$ if$v_1 = 0, v_2 = 0 and\ \rho = 0.$ Hence, the severity of outbreak will be lower when $R_0{}^q > 1$ than when $R_0 > 1$ .The above inequalities hold from the elementary algebra since $\delta(\mu + \mu_c + v_2 + \rho + \gamma) \geq \delta(\mu_d + \mu_c + \gamma)$.

Finally, the summary of the results of analysis of disease-free equilibrium states is that the disease-free equilibrium of the system of equations (3) – (5) is locally asymptotically stable if $R_0{}^q < 1$; whereas it is unstable, with a lower outbreak growth rate than that of the original no-control model whenever $R_0{}^q > 1$.

Endemic dynamics

Assuming that the disease-free equilibrium of the extended model is unstable and the disease is sustained in the population then there is need to investigate the long-term behavior of the disease dynamicsfor $R_0{}^q > 1$.

Suppose the endemic equilibrium of the model equations (3) - (5) is denoted by

$$E^* = (S^*, I^*, B^*) \quad (15)$$

Where and represent the population of each compartment at endemic equilibrium. Hence, the model equations (3) – (5) are written in terms of the endemic state as

$$\pi - \mu S^* - \frac{\beta_1 B^*}{B^* + \aleph} S^* - \beta_2 I^* S^* - v_1 S^* = 0 \quad (16)$$

$$\frac{\beta_1 B^*}{B^*+\aleph} S^* + \beta_2 I^* S^* - (\mu + \mu_c + v_2 + \rho + \gamma) I^* = 0 \quad (17)$$

$$\varepsilon I^* - \delta B^* = 0 \quad (18)$$

Note that σR is dropped in eqn. (16) due to the fact that the compartment R is not included in the model analysis as stated earlier under eqn. (6)

From eqn. (18),

$$B^* = \frac{\varepsilon I^*}{\delta} \quad (19)$$

Solving for the remaining compartments at endemic equilibrium (i.e. $S^*$and I^*), their values are positive since each compartment and parameter is assumed non-negative.

Local asymptotic stability of the endemic equilibrium

Theorem 1: The endemic equilibrium state E^* is locally asymptotically stable if $R_0{}^q > 1$.

The linearization approach shall be employed to investigate the stability of the endemic equilibrium state E^*.The approach shall be employed to show that the endemic equilibrium state E^* is locally asymptotically stable. To achieve this, eqn. (11) is used, so that, substituting B^* for B and S^* for S and replacing $\frac{\beta_1 B^*}{B^*+\aleph} + \beta_2 I^* > 0$ by M and $\frac{\beta_1 \aleph S^*}{(B^*+\aleph)^2} > 0$ by N, the Jacobian matrix eqn. (11) is reduced to

$$J(E^*) = \begin{bmatrix} -M-(\mu+v_1) & -\beta_2 S^* & M+N+\beta_2 I^* \\ M & \beta_2 S^* - (\mu+\mu_c+v_2+\rho+\gamma) & M-N+\beta_2 I^* \\ 0 & \varepsilon & -\delta \end{bmatrix} \quad (20)$$

The characteristic equation in λ of eqn. (20) is evaluated as follows

$$(M+\mu+v_1+\lambda)[(\lambda+\delta)[-\beta_2 S^* + (\mu+\mu_c+v_2+\rho+\gamma+\lambda)] - \varepsilon(M-N+\beta_2 I^*)] = 0 \quad (21)$$

On simplification, eqn. (21) can be written as

$$a_0\lambda^3 + a_1\lambda^2 + a_2\lambda + a_3 = 0 \quad (22)$$

Where

$$a_0 = 1$$

$$a_1 = M + 2\mu + \mu_c + v_1 + v_2 + \rho + \gamma + \delta$$

$$a_2 = (M+\mu+v_1)(\mu+\mu_c+v_2+\rho+\gamma+\delta) + \delta(\mu+\mu_c+v_2+\rho+\gamma-\beta_2 S^*) - \varepsilon(M-N+\beta_2 I^*)$$

$$a_3 = (M+\mu+v_1)(\delta(\mu+\mu_c+v_2+\rho+\gamma-\beta_2 S^*) - \varepsilon(M-N+\beta_2 I^*))$$

The Routh-Hurwitz criterion inTian*et al.*(2010) and Liao and Wang (2011) requires

$$a_1 > 0,\ a_2 > 0,\ a_3 > 0 \text{and}$$

$$a_1 a_2 - a_0 a_3 > 0 \quad (23)$$

as the necessary and sufficient conditions for the local asymptotical stability of the endemic equilibrium of the model; i.e., all the solutions of eqn. (22) must have negative real parts.

$a_1 > 0$is obvious. Meanwhile, to establish the validity of eqn. (23) for the local asymptotic stability of the extended model, eqn. (17) and eqn. (19) shall be considered and eqn. (19) will be substituted into eqn. (17) to obtain

$$(\mu + \mu_c + v_2 + \rho + \gamma) = \beta_2 S^* + \frac{\beta_1 S^* \varepsilon}{\varepsilon I^* + \aleph\delta} \quad (24)$$

From (24),

$$(\mu + \mu_c + v_2 + \rho + \gamma) - \beta_2 S^* > 0 \quad (25)$$

Since all the model parameters as well as M and N are positive andeqns (24) and (25) hold then all the inequalities in (23) are true. Hence, the endemic equilibrium of the extended model is locally asymptotically stable. The implication of the local asymptotical stability of the endemic equilibrium state $E^* under R_0{}^q > 1$ as proved above is that even though the prevention and control measures are not strong enough to remove the

epidemic, they have the effect of reducing the size of the infection, particularly for the long-term disease dynamics. We expect that when I^* is close to zero, an endemic state would be unlikely to occur or persist in reality, since practical endemism requires a reasonably higher value for I^* (Tian *et al.*, 2010)

Results and Discussion

In our analysis, there exists a disease free equilibrium state and theendemic equilibrium state. We established that if$R_0{}^q$ <1 then disease free equilibrium state is locally asymptotically stable, which implies that the prevention and control measures are potent enough to inhibit the emergence of secondary infections. The United States of America is one of the several countries that has been maintaining stability in terms of cholera outbreak both locally and globally for more than a century. Even though there are occasional sporadic cases of cholera resulting from several people who traveled abroad to countries where cholera is endemic and contracted the disease either by drinking the water or eating some food that was contaminated and developed illness on returning to the United States but at large, no secondary transmission has been recorded within the United States. We also established that an endemic equilibrium state exists if $R_0{}^q$ >1 which implies that the prevention and control measures are not strong enough to break the chain of transmission of the disease and the population experienced mild waves of cholera epidemic. The frequent outbreak of cholera in most developing countries of the world is as a result of carefree attitude towards cholera prevention and control. Despite availability of cholera measures in these countries, the measures are being handled with levity hands.

Conclusion

In this work we modified the model by Fung [11] to incorporate vaccination and therapeutic treatment as prevention and control strategies against cholera transmission. We derive the basic reproduction number and conduct a careful equilibrium and stability analyses. Both the disease free equilibrium state and the endemic equilibrium state are found to be locally asymptotically stable. From the results obtained from the study we conclude that the most effective way to curb cholera outbreak is to ensure the effectiveness and wide coverage of cholera vaccination as well as cholera treatment through the use of drugs in cholera endemic regions. The availability and potency of these interventions are capable of averting 120 000 deaths due to cholera yearly.

References

1. Azman, A. S., Rudolph, K. E., Cummings, D. A. T., Lessler, J. (2012). The incubation period of cholera: A system review. Journal of Infection, 66, 432-438.
2. Mukandavire, Z., Liao, S., Wang, J., Gaff, H., Smith, D. L. and Morris, J. G. Jr (2011). Estimating the reproductive numbers for the 2008-2009 cholera outbreaks in Zimbabwe. Proc. Natl Acad. Sci. USA, 108(21), 8767- 8772.
3. Fakai, S. A., Ibrahim, M. O. and Siddiqui, A.M.(2014). A

deterministic model on cholera dynamics and some control strategies. International Journal of Scientific Engineering and Technology, 3(8), 1115-1118.

4. Posny, D. and Wang, J. (2014). Modeling cholera in periodic environments.Journal ofBiological Dynamics, 8(1), 1-1

5.World Health Organisation, (2012).Global Task on Cholera Control. Cholera Country Profile: Nigeria. Retrieved from: http:/www.who.int/cholera countries/Nigeria country profile 2011.pdf

6. Fatima,S., Krishnarajah, I., Jaffar, M. Z. A. M., Adam, M. B. (2014). A mathematical model for the control of cholera in Nigeria. Research Journal of Environmental and Earth Sciences,6(6), 321 – 325.

7. Grad, Y. H., Miller, J. C. and Lipsitch, M. (2012).Cholera modeling: challenges to quantitative analysis ans predicting the impact ofintervention. Epidemiology, 23(4), 523-530.

8. Chao, D. L., Holloran, M. E. Longini, I. M. Jr. (2011). Vaccination strategies for epidemic cholera in Haiti with implications for the developing world.Proc. Natl Acad. Sci. USA, 108,7081-7085.Azman,

9. Azman, A. S., and Lessler, J. (2014). Reactive vaccination in the presence of disease hotspot.Pro.R. Soc. B. http:/rspb.royalsocietypublishing. org Emerging themes in epidemiology. htpp://www.et online.com./content/11/1/1.

10.Me'decinsSanFrontie'res (MSF, 2012). Oral cholera vaccines highly effective during outbreak in Guinea.Retrieved from: http:/www.msf.org.

11 Fung, I. C-H.(2014). Cholera transmission dynamic models for public health practitioners. Fung

12.Wang, J. and Modnak, C. (2011).Modeling Cholera Dynamics with Controls.Canadian Applied Mathematics Quarterly.19(3), 255-273

13. Tian, J. P., Liao, S. and Wang, J. (2010). Dynamical Analysis and Control Strategies in Modelling Cholera.Retrieved from:ath.wm.edu/jptian/tain-liao-wang.

14. Tian, J. P. and Wang, J. (2011), Global Stability for Cholera Epidemic Models. Mathematical Biosciences 232, 31-41.

15. van den Driessche, P. and Watmough, J. (2002). Reproduction number and sub – threshold endemic equilibria for compartmental models of disease transmission.Math.Biosci. 180,29 – 48.

16.Tien, J. H. and Earn, D. J. D. (2010). Multiple transmission pathways and disease dynamics in a waterborne pathogen model.Bull. Math.Biol.72, 1502 – 1533.

.

Covenant Journal of Physical & Life Sciences (CJPL) Vol. 6 No. 1, June, 2018

An Open Access Journal available online

Phytochemical and Antimicrobial Properties of *Mangifera indica* Leaf Extracts

Olasehinde G. I.,[1] Sholotan K. J.,[1,2] Openibo J. O.,[1] Taiwo O. S.,[1] Bello O. A.,[1] Ajayi J. B.,[2] Ayepola O. O.[1] & Ajayi A. A.[1]

[1]Department of Biological Sciences, Covenant University, Ota, Ogun State, Nigeria
[2]Ogun State College of Technology, Igbesa, Nigeria.
grace.olasehinde@covenantuniversity.edu.ng

Abstract: There have been reports of increasing development of drug resistance among human pathogens as well as undesirable side effects of certain antimicrobial agents.It is therefore necessary to search for new agents that are better, cheaper and without side effects for treating infectious diseases especially in developing countries. In this study, phytochemical composition and antimicrobial activities of aqueous and ethanolic extracts of leaves of *Mangifera indica* were investigated. Standard methods were employed to screen for the phytochemicals. Agar well diffusion method was used to determine the antimicrobial effects of aqueous and ethanolic extracts of *M. indica* leaves against seven different clinical isolates namely:*Stapylococcus aureus*, *Micrococcus virians*, *M. leteus*, *Escherichia coli*, *Klebsellia pneumoniae*, *Pseudomonas aeruginosa* and a fungus, *Candida albicans*. Phytochemical screening showed the presence of active pharmacological components such as tannins, saponins, cardiac glycoside, flavonoid and alkaloids. Aqueous extract demonstrated a higher activity than the ethanolic extract. *S. aureus* showed highest sensitivity to the aqueous extracts with MIC 31.25mg/mL. Least sensitivity was observed in *K. pneumoniae* and *Candida albicans* with MIC 125mg/mL each in the two extracts.*M. indica* exhibited significant antimicrobial activity comparable to gentamicin which is used as control in this study.

Keywords: Resistance, Antimicrobial, Phytochemicals, Sensitivity

Introduction

Continuous spread of infectious diseases is a major apprehension for health institutions, pharmaceutical companies and government think-tanks all over the world. Failure of treatment, particularly with the current escalating trends of multi-drug

resistance (MDR) to the available modern drugs or antibiotics among emerging and re-emerging bacterial pathogens leads to serious risks [1].

Prior to this century, medical practitioners whether allopath (medical doctors), homeopaths, naturopaths, herbalists or shamans had to know the plants in their areas and how to use them since many of their drugs were derived from plants [2–5]. Around 1900, 80% of the drugs were derived from plants, however, in the decades that followed, the development of synthetic drugs from petroleum products caused a sharp decline in the pre-eminence of drugs from live plant sources [6–8]. However, with the recent trend of high percentage resistance of microorganisms to the present day antibiotics, efforts have been intensified by researchers towards a search for more sources of antimicrobial agents [1, 9].

Mangifera indica is commonly called mango (English), manako (Hawai‘i), manggo’am (Fiji), tharyetthi (Myanmar), mangot, mangue or manguier (French), aam, am or amb (Hindi), bobbiemanja, kanjannamanja, magg, manggaboomormanja (Dutch), mamung (Thailand), manga or mango (Spanish), manga (Portuguese), manga, mempelamorampelam (Malaysia), manggaor mempelamn (Indonesia), mangobaum (German), paho (Philippines) and xoài (Vietnam), mongoro (Yoruba, Nigeria), mangolo (Igbo, Nigeria) and mangoro (Hausa, Nigeria). The fruits are eaten and used in the production of juice and wine. Traditionally, the mango plant has medicinal applications.Mango extract has been reported to have anti malaria effect by Tsabang *et al* [10] and was found to display *in vitro* activity against *Plasmodium falciparum* [11].

The leaves of *M. indica*have also been reported to possess antibacterial activity [12]. Ojewole [13] reported the anti-inflammatory, analgesic and hypoglycemic effects of *M. indica* stem-bark aqueous extract. Doughari and Manzara [12] also affirm that both acetone and methanol extracts inhibited the growth of gram positive bacteria, with acetone extract exerting more activities on all the gram positive bacteria with zone of inhibition between 15 - 16 mm, and a gram negative bacterium *Salmonella typhi* (14 mm) at 250 mg/ml. Stem bark of *M. indica* showed significant antibacterial and antifungal activities against *Streptococcus pneumoniae*, *Enterobacter aerogenes*, *Klebsiella pneumoniae* and *Candida albicans* with MIC of 0.08 mg/ml [14]. *Mangifera indica* contains alkaloids and glycosides which are of great importance pharmacologically. Certain aliphatic constituents such as coumarin, mangiferin, sequiterpinenoids, triterpinoids and phenolics have also been reported from the stem barks of different cultivars of *M. indica* [15]. It is believed that the presence of these phytochemicals confers on *Mangifera indica*, its medicinal ability.

Studies have shown that aqueous and ethanolic herbal extracts show less toxicity in animal models than N-Haxane, acetone, ethanol and other solvents [1].This study therefore investigated and revalidated the phytochemical and *in vitro*antimicrobial properties of aqueous and ethanolic extracts of *Magniferaindica.*

Methods

Sampling: Samples of *Mangifera indica* (leaves) were obtained from Igbesa in Ado Odo/Otta Local Government Area of Ogun State and were identified in the Department ofBiological Sciences, Covenant University, Ota, Ogun State, Nigeria.

Preparation of plant materials: Freshly collected leaves of *M. indica*were washed with distilled water and dried under the shade at normal room temperature for 10 days. After drying, the plant material was pounded using mortar and pestle into smaller particles and then blended to powder using an electric blender. 200grams of the powdered samples were stored in airtight containers and kept under normal room temperature for further screening.

Collection of test organisms: Clinical isolates of *Escherichia coli*, *Pseudomonas aerugenosa,Micrococcus leteus,Staphylococcus aureus*, *Klebsiellapneumoniae*, *Micrococcus virians* and *Candida albicans* were collected from Microbiological Teaching Laboratory of Covenant University Ota in Ado OdoOta Local Government Area of Ogun State, Nigeria. The collected isolates were sub-cultured for 24hours and were adjusted to 0.5McFarland standard.

Preparation of aqueous extracts: Samples **(**100 g) of the dried powdered of the plant leaves were soaked in1000 ml of distilled water contained in a 2000 ml flask. The flask was plugged with cotton wrapped with foil and then allowed to stand for 48 hours. The suspension was shaken vigorously and filtered using a muslin cloth. The filtrates wereconcentrated using a rotary evaporator. The concentrated extract was stored in airtight sample bottle until required. For the preparations of crude extracts for antimicrobial screening, the extract wasreconstituted in Dimethyl Sulphoxide (DMSO) to500mg, 250mg, 125mg and 62.5mg/ml by dissolving 0.5g in 1ml, 0.5g in 2ml, 0.5g in 4ml and 0.5g in 8ml DMSO respectively.

Preparation of ethanolic extracts: Samples **(**100 g) of the dried powdered of the plant leaves were soaked in 1000 ml of ethanol containedina 2000ml flask. The flask was plugged with cotton wrapped with foil and then allowed to stand for 72 hours. The suspension was shaken vigorously and filtered using a muslin cloth. The filtrates wereconcentrated using a rotary evaporator. The concentrated extract was stored in airtight sample bottle until required. For the preparations of crude extracts for antimicrobial screening, the extract was reconstituted in Dimethyl Sulphoxide (DMSO) to 500mg, 250mg, 125mg and 62.5mg/ml by dissolving 0.5g in 1ml, 0.5g in 2 ml, 0.5g in 4ml and 0.5g in 8ml respectively.

Phytochemical screening: Phytochemical tests for the screening and identification of bioactive chemical constituents in the medicinal plants under study were carried out on the extract using the standard procedures as previously described [16].

Qualitative analysis of phytochemical constituents

***Tannins*:** The powdered leaf sample (0.5 g) was boiled in 20 ml of distilled water in a test tube and filtered, 0.1% $FeCl_3$was added to the filtered samples and observed for brownish green or a

blue black colouration which shows the presence of tannins.

***Saponins*:** The powdered leaf sample (2.0 g) was boiled in 20ml of distilled water in a water bath and filtered off; the filtratewas mixed with 5ml of distilled water in a test tube and shaken vigorously to obtain astable persistent froth. The frothing is then mixed with 3drops of olive oil and for the formation of emulsion which indicates the presence of saponins.

***Flavonoids*:** A few drop of 1% NH_3solution was added to the aqueous extract of each plant sample in a test tube. A yellow coloration is observed if flavonoids compound are present.

Glycosides: Concentrated H_2SO_4 (1 ml) was prepared in a test tube, 5 ml of aqueous extract from the powdered leaf samplewas mixed with 2ml of glacial CH_3COOH containing 1 drop of $FeCl_3$. The above mixture was carefully added to 1ml of concentrated H_2SO_4so that the concentrated H_2SO_4 settled beneath the mixture. The presence of cardiac glycoside constituent was indicated by appearance of a brown ring.

***Alkaloids*:** The plant sample (5.0 g) was prepared in a beaker and 200ml of 10% CH_3CO**O**H in C_2H_5OH was added to the plant sample nearly 0.5g.

Antimicrobial activity: Agar well diffusion technique as described by Olasehinde*et al*. [1] was adopted for the study. 56 petri-dishes filled with 20ml of Mueller Hinton Agar each (MHA Oxoid) was inoculated with 0.5Mcfarland's standard of each test organisms using sterile swab stick as demonstrated by Cheesbrough[16]. Duplicate well of 7mm diameter were bored on each plate using sterile cork borer and filled with equal volume of plant extracts (0.4ml) with the aid of a sterile micropipette. Control experiment was done using commercially produced Gentamicin.The plates were incubated at 37^{o}C for 18-24hours. Zones of Inhibition were measured in millimeter (mm) and the average values were calculated and recorded.

Determination of minimum inhibitory concentration (MIC): The determination of Minimum Inhibitory Concentration (MIC) was carried out on the extract against the test isolates *(E. coli, K. pneumoniae, M. viridans, M. leteus, S. aureus, P. aeruginosa and C. albicans)* due to its sensitivity against the growth of the isolates. Nutrient broth (5 ml) was dispensed into each of the 56 test-tubes and sterilized at 121^{o}C for 15 minutes and allowed to cool to 40-45^{o}C. 0.5ml of 0.5Mcfarland standard of each test isolates were introduced into 8 different tubes while 5ml of each extract concentrations (500, 250, 125, and 62.5 mg/ml of aqueous and ethanolic extract) were introduced into 7 different tubes containing each isolates, labelled accordingly and incubated at 37^{o}C for 24 hours.

Results and Discussion

The preliminary phytochemical tests carried out on the aqueous leaf extract showed the presence of tannin, saponins, alkaloids and cardiac glycosides but sterols and flavonoids were absent. In the ethanolic extract, saponin, tannin, flavonoids, alkaloids and cardiac glycosides were all present but sterols was absent (Table 1).

Table 1: Phytochemical properties of *M. indica* leaf extracts

Phytochemicals	Leave Extract	
	Aqueous	Ethanolic
Tannin	+	+
Saponin	+	+
Sterols	-	-
Flavonoids	-	+
Alkaloids	+	+
Cardiac glycosides	+	+

Antimicrobial activity of aqueous and ethanolic extracts of M. indica leaf assayed against seven human pathogenic microorganisms, using gentamicin as positive control showed great potency at varying concentration (Table 2). Phytochemical screening of the extracts of M. indicashowed presence of active pharmacological components such as tannins, saponins, cardiac glycoside, flavonoid and alkaloids. This observation agrees with the findings of Madunagu et al. [17]. These components are known to be biologically active because they protect the plant against infections and predations by animals. Phytochemicals generally exert their antimicrobial activities through different mechanisms from that of synthetic drugs [18].

The leaves and flowers of M. indica have been reported to possess antibacterial activity against E. coli and other bacteria in the family Enterobacteriaceae and the bioactive component mangiferin isolated from M. indicawas reported to possess remarkable anti-influenza activity [19]. The presence of phyto-constituents in the leaf extracts may be responsible for the antibacterial activity of the plant [20–22]. Medicinally, this is important for the treatment of pneumonia, asthma and inflamed tissues.It also plays important roles in herbs for treating dysentery [23]. This justified the use of M. indica in traditional medicine.

The antibacterial assay performed using the Agar well diffusion method showed the clear zones of inhibition in diameters. Table 2 above showed the varied susceptibility of the bacteria and fungi used as test organisms in this study.The susceptibility exhibited are dependent on the microorganisms and extracting solvents. This agrees with earlier findings that length of zones of growth inhibition from different studies vary from one organism to another, plants and concentration difference [24, 25]. The patterns organisms which were sensitive tend to move away from the region around the extract while those that are resistant show no zones of inhibition of growth. In this study, it was observed that the aqueous extract demonstrated a slightly higher activity atsome concentrations than the ethanolic extract. Ethanolic extract was observed to possess more potency against P. aerugenosa and M. virians with zones of inhibition value of 21 mm and 50 mm respectively as shown in Table 2.

Table 2: Antimicrobial activity of aqueous and ethanolic leaf extracts of M. indica

Test isolates	Aqueous extracts in mg/ml and Zone of Inhibition (mm)				Control Gentimicin (ug)	Ethanolic extracts in mg/ml and zones of Inhibition (mm)			
	500	250	125	62.5	20	500	250	125	62.5
S. aureus	*25*	*20*	*18*	*15*	*20*	*20*	*15*	*15*	*10*
M. leteus	*20*	*15*	*10*	*10*	*12*	*20*	*15*	*12*	*10*
K. pneumoniae	*24*	*15*	*10*	-	*21*	*21*	*10*	*10*	-
P. aerugenosa	*20*	*18*	*16*	*15*	*12*	*21*	*20*	*12*	*10*
E. coli	*25*	*20*	*15*	*12*	*20*	*22*	*18*	*16*	*12*
M. virians	*30*	*25*	*16*	*12*	*20*	*50*	*20*	*11*	*10*
C. albicans	*25*	*15*	*12*	*10*	*10*	*20*	*14*	*12*	*10*

- = No zone of inhibition

Table 3: Minimum inhibitory concentration of aqueous and ethanolic leaf extracts of *M. indica* against test isolates

Test isolates	*Aqueous extracts in mg/ml and MIC*					*Ethanolic extracts in mg/ml and MIC*				
	500	*250*	*125*	*62.5*	3	*500*	*250*	*125*	*62.5*	3
S. aureus	-	-	-	-		-	-	-	+	
M. leteus	-	-	+	+		-	-	+	+	
K. pneumoniae	-	-	+	+		-	+	+	+	
P. aerugenosa	-	-	-	-		-	-	+	+	
E. coli	-	-	-	+		-	-	-	+	
M. virians	-	-	-	+		-	-	+	+	
C. albicans	-	-	+	+		-	+	+	+	

Key: - = No growth (no turbidity); + = Growth (turbidity)

Aqueous extract had better potency against S. aureus at all concentrations while gentamicin gave an inhibition zone of 20 mm similar to that of aqueous extract at 250 mg/ml and ethanolic extract at 500 mg/ml. For M. leteus, both extracts had similar effects while gentamicin had zone of inhibition of 12 mm which is similar to that ethanolic extract at 125 mg/ml. Furthermore, aqueous extract showed a greater potency against K. pneumoniae at all concentrations.

Ethanolic extract established a better effect at all concentrations against P. aerugenosa while gentamicin has a zone of inhibition of 12 mm, an effect shown by 125 mg/ml of ethanolic extract. From the same table, it is obvious that aqueous extract had a better potency between the two extracts against E. coli while gentamicin had similar effect of 20 mm with 250 mg/ml of ethanolic extract.

Assessing the zones of inhibition against M. virians, it is obvious that ethanolic extract had a better effect of 50 mm at 500 mg/ml but at other concentrations aqueous extract had the

activity against the same organism while Gentamicin had an inhibition zone of 20 mm, a zone size also shown at 250 mg/ml of ethanolic extract. Aqueous extract had better potency against C. albicans at all concentrations while gentamicin had inhibition zone of 10 mm, inhibition zone size shown by 62.5mg/ml of both extracts. Aqueous extract of M. indica had minimum inhibitory concentration (MIC) of 62.5 mg/ml against S. aureus and P. aerugenosa only while an MIC of 31.25 mg/ml was observed for M. leteus, K. pneumoniae, and C. albicans had turbity. The MIC for K. pneumoniae, and C. Albicans was found to be 62.5 mg/ml and 125 mg/ml for S. aureus and E. coli respectively.

The zones of inhibition and MIC of M. indica extracts observed in this study compares with earlier findings where zones of inhibition ranging between 12 mm and 16 mm were recorded for extracts of M. indica stem bark and leaves for Gram negative and Gram positive bacteria [13]. Doughari and Manzara [12] found that both acetone and methanol extracts inhibited the growth of gram positive bacteria, with acetone extract exerting more activities on all the Gram positive bacteria with zone of inhibition between 15 - 16 mm, and a Gram negative bacterium Salmonella typhi (14 mm) at 250 mg/ml. Stem bark of M. indica had been found to show significant antibacterial and antifungal activities against Streptococcus pneumoniae, Enterobacter aerogenes, Klebsiella pneumonia and Candida albicans with MIC of 0.08 mg/ml [6].

This study has established that crude aqueous and ethanolic extracts of M. indica leaves have good activity against Gram positive and negative bacteria and the fungus, Candida albicans at low concentrations.

References

1 Olasehinde G. I. , Okolie Z. V., Oniha M. I., Adekeye B. T. and A. A. Ajayi (2016). In vitro antibacterial and antifungal activities of Chrysophyllum albidum and Diospyros monbuttensis leaves,J. Pharm. Phytothera. 8 (1):1–7.

2 Aderibigbe A. O., Emudianughe T. S. and Lawal B. A. (2001). Evaluation of the antidiabetic action of Mangifera indica in mice. Phytothera. Res. 15(5):456–458.

3 Aderibigbe A. O., Emudianughe T. S. and Lawal B. A. (1999). Antihyperglycaemic effect of Mangifera indica in rat. Phyto. Res.13(6) :504–7.

4 Zheng M. S. and Lu Z. Y. (1990). Antiviral effect of mangiferin and isomangiferin on herpes simplex virus.,Chi. Med. J.103(2):160–165.

5 Zhu X. M., Song J. X.,Huang Z. Z., Wu Y. M. and Yu M. J. (1993). Antiviral activity of mangiferin against herpes simplex virus type 2 in vitro. Zhongguo yao li xue bao, 14(5): 452–454.

6 Singh M., Khatoon S., Singh S., Kumar V., Rawat A. K. S. and Mehrotra S. (2010). Antimicrobial screening of ethnobotanically important stem bark of medicinal plants. Pharma. Res. 2(4), 254–257.

7 Scartezzini P. and Speroni E. (2000). Review on some plants of Indian traditional medicine with antioxidant activity. J. Ethnopharma. 71(1–2):23–43.

8 Sofowora A. O. (1993).Medicinal plants and traditional medicine in Africa. University of Ife Press 2nd ed. pp 320.

9 Barie P. S. (2012). Multidrug-Resistant Organisms and Antibiotic Management.Surg. Clin. N. Amer. 92(2):345–391.

10 Tsabang N., Fokou P. V. T., Tchokouaha L. R. Y., Noguem B., Bakarnga-Via I., Nguepi M. S. D. et al. (2012).Ethnopharmacological survey of Annonaceae medicinal plants used to treat malaria in four areas of Cameroon. J. Ethnopharma.. 139(1):171–180.

11 Rasoanaivo P.Ramanitrahasimbola D., Rafatro H., Rakotondramanana D., Robijaona B.,Rakotozafy A. et al.(2004). Screening extracts of Madagascan plants in search of antiplasmodial compounds. Phytothera. Res.18(9):742–747.

12 Doughari J. H. and Manzara S. (2008). In vitro antibacterial activity of crude leaf extracts of Mangifera indica Linn. Afr. J. Microbiol. Res.(2):67–72.

13 Ojewole J. (2005). Anti-inflammatory, analgesic and hypoglycaemic effects of Mangifera indica Linn. (Anacardiaceae) stem-bark aqueous extract," Meth. F. Expt. Clin. Pharma. 27(8): 547.

14 Singh N., Kumar M. and R. K. Singh R, K. (2012). Leishmaniasis: Current status of available drugs and new potential drug targets," Asian Pac. J. Trop. Med. 5(6):485–497.

15 Ghosal S. and Chakrabarti D. K. (1988). Differences in phenolic and steroidal constituents between healthy and infected florets of Mangifera indica.Phytochem. 27(5):1339–1343.

16African Networks on Ethnomedicines (2004). African journal of traditional, complementary, and alternative medicines. [African Networks on Ethnomedicines], 2004.

17 Madunagu B., Ebana R. and Ekpe E. (1990). Antibacterial and antifungal activity of some medicinal plants of Akwa Ibom state.West Af. J. Biol. Appl. Chem. 35: 25-30.

18 Scalbert A. (1991). Antimicrobial properties of tannins.Phytochem,30(12):3875 -3883.

19 Poongothai P. and Rajan S. (2013). Antibacterial Properties of Mangifera indica flower extracts on Uropathogenic Escherichia coli.Intl.J. Curr.Microbiol. Appl. Sci. 2(12):104-111.

20 KhanM. A. and Khan M. N. I. (1989). Alkyl gallates of flowers of Mangifera Indica" Fitoterapia. 60:284.

21 Khan M. N. I., Nizami S. S., Khan M. A. and Ahmed Z. (1993).New saponins from Mangifera indica.J. Nat. Prod. 56(5):767-770.

22 Cowan M. M. (1999). Plant products as antimicrobial

agents," Clin.l Microbiiol Rev.12(4):564-582.

23 Leven M.,Vanden Berghe D., Mertens F., Vlietinck A. and LammensE. (1979).Screening of higher plants for biological activities I. Antimicrobial activity.Planta.Med. 36(4): 311-321.

24 El-Mahmood A. M., Doughari J. H. and Ladan N. (2008). Antimicrobial screening of stem bark extracts of Vitellaria paradoxa against some enteric pathogenic microorganisms. Afr. J. Pharm. Pharmacol. 2(5):89-94.

25 Mann A., Banso A. and Clifford L., (2008). An antifungal property of crude plant extracts from Anogeissus leiocarpus and Terminalia avicennioides," Tanz. J Health Res.10(1):34-38.

Covenant Journal of Physical & Life Sciences (CJPL) Vol. 6 No. 1, June, 2018

An Open Access Journal available online

Theoretical Investigation of Temperature and Grain Size Dependence of Thermal Properties of alpha-Silicon Crystal

Nenuwe O.N.

Department of Physics, Federal University of Petroleum Resources,
P. M. B. 1221, Effurun, Delta State, Nigeria
nenuwe.nelson@fupre.edu.ng

***Abstract*:** Using reverse non-equilibrium molecular dynamics method, we study the thermal properties of grain boundary between two alpha-silicon crystal grains with (200) and (220) crystallographic orientations. The interfacial thermal conductance of the grain boundary and thermal conductivity are temperature dependent, leading to increasing/decreasing thermal transport as the temperature is increased. Also, thermal conductivity increased with increasing grain size. The observed decrease in thermal resistance indicates the suitability of silicon as interface materials for high-thermal conductivity material applications and thermal management in micro and nanoelectronic devices.

Introduction

The desire for faster and cheaper electronic devices, continuous device miniaturization and increasing density of components on an integrated circuit has increased the complexity of micro- and nanoelectronics [1– 6]. It is well known that downsizing of electronic devices has enhanced computing capabilities at the expense of increasing heat dissipation across the material [7–9]. This has posed great thermal management challenge within the electronic device industry. Over the past fifty years [10], it has motivated material scientists and engineers into rigorous research and continuous development of new materials, by making thermal designs an integral part of the fabrication of electronic devices to increase computing performance. For example,

in some processor modules, the power required for high-performance computing (HPC) may reach 300 – 400W resulting to heat loads up to 4kW for processors in a ten-socket computing system [11]. High management of power dissipation has great implications on such systems, and therefore, requires good thermal management solutions that will quickly transfer the heat from hot spots to regions of low temperature to maintain high reliability of such electronic device. According to Panasonic [12], energy consumption rate keeps increasing even as the size of electronic devices is continuously decreasing, and the usual techniques for thermal transfer have failed to meet the present day electronic designs. Hence, they developed the Pyrolytic graphite sheet (PGS) for thermal management solutions. The PGS was designed to diffuse heat generated by heat sources like power amplifier, computer processors, and batteries. Also, Tang et al. [13] reiterated that thermal interface materials which are usually introduced to bridge the gap between difficulties to minimize the thermal contact resistance can capably improve heat dissipation of electronic devices [14]. It is important to note that thermal conductivity is difficult to predict when the electronic device is fabricated from different materials. Therefore, material scientists and engineers are always designing interfaces between materials to minimize or maximize thermal conductivity [15].

Thus, in this review article, we use the reverse non-equilibrium molecular dynamics (RNEMD) [16] with a classical potential to simulate the heat flow through alpha-silicon (200) and (220) interface and calculate the interfacial Kapitza conductance and resistance of the grain boundary at different temperatures. The thermal conductivity is calculated at all temperatures, and the grain- size dependence of thermal conductivity is also investigated to have more insight into the behavior of thermal conductivity as the grain size is varied.

This article is arranged as follows: Section 2 briefly reviews the theory of RNEMD and discusses the computational details. The results obtained are analyzed in Section 3, and Section 4 discusses the conclusion of the study.

Theory and Computational methods

The interfacial thermal conductance is calculated with the reverse non-equilibrium molecular dynamics method. In this method heat flux *dQ/dt* is imposed through two alpha-silicon crystal grains with (200) and (220) crystallographic orientations, which results in temperature jump (ΔT) across the grain boundary since the interface creates additional thermal resistance, R to the heat flow, and a temperature gradient is generated over the hot and cold grains as illustrated in Figure 1. The thermal conductance (G) across an interface, also called Kapitza conductance [17] is directly proportional to the heat flux and inversely proportional to the temperature jump developing across the grain boundary as given by Eq. (2.1)

$$G = \frac{dQ/dt}{\Delta T} = \frac{1}{R} \qquad (2.1)$$

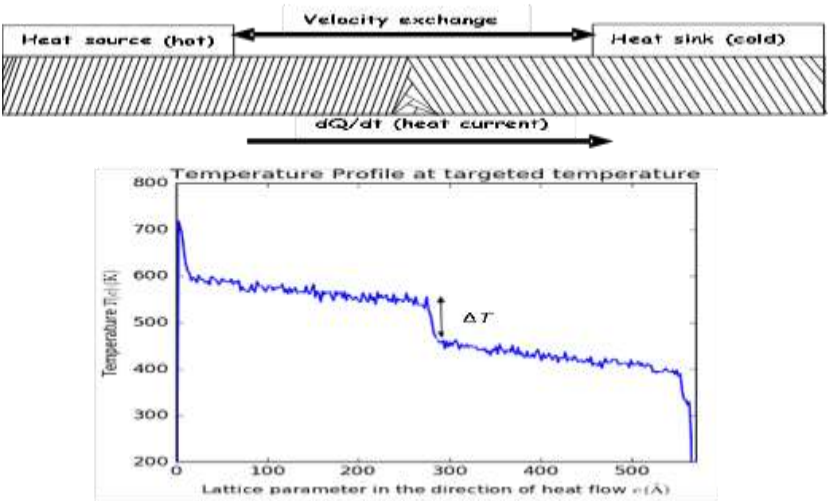

Figure 1. A diagram of simulation system for determining thermal conductivity across the interface of two silicon crystals in (200) and (220) crystallographic orientations in the regime of RNEMD technique.

In Figure 1, the heat flux is imposed by periodically exchanging the positions and velocities of the hottest atoms in the heat sink (cold grain) and coldest atoms in the heat source (hot grain). After the exchange, the velocities of the atoms in the cold and hot grains are given as [18]

$$\mathrm{v}_c' = -\mathrm{v}_c + 2\left(\frac{m_c\mathrm{v}_c + m_h\mathrm{v}_h}{m_c + m_h}\right) \qquad (2.2)$$

$$\mathrm{v}_h' = -\mathrm{v}_h + 2\left(\frac{m_c\mathrm{v}_c + m_h\mathrm{v}_h}{m_c + m_h}\right) \qquad (2.3)$$

Where v_c and v_h are velocities of atoms before the exchange, v'_c and v'_h are velocities after the exchange in the cold and hot grains, m_c and m_h are the respective masses for the cold and hot atoms. This results in heat flow from the heat source to the heat sink. Because of energy conservation and the buildup of a temperature gradient, energy transport is generated in the opposite direction. When adequate exchange has occurred, a steady-state heat flux, dQ/dt is reached in the system, and it is directly proportional to the magnitude (but opposite in direction) of the temperature gradient, dT/dz as given by Eq. (2.4). Where κ, is the thermal conductivity of the material, and A, is the area perpendicular to heat flux.

$$\frac{dQ}{dt} = -\kappa A\frac{dT}{dz} \qquad (2.4)$$

In this study, the virtual nanolab 2017.1 [19] is used to prepare grain boundary between two α-silicon (Si) crystal grains with (200) and (220) crystallographic orientations. The thermal current is directed to run along the z-direction. The (200) and (220) crystal grain interface are studied for (A_xXB_yXC_z=) 11.52X11.52X570, 11.52X11.52X680, 15.3601X15.3601X270 and 15.3601X15.3601X550 supercells. The C_z-vector was chosen to be larger than A_x and$B_y$because in the non-equilibrium thermal current simulations, it is customary to choose a large cell length in the direction of heat flow. The supercell created is

non-periodic in the C_z-direction so as to terminate the system by vacuum at either end. Then, the slab is centered in the middle of the supercell.

The atomistix toolkit (ATK) force field calculator [19-21] and Stillinger-Weber potential [22] are used for the equilibration of the system. The system is first optimized using LBFGS method [23] with a tolerance of 0.1eV/A and 0.1GPa in stress error, to remove initial large destabilizing forces that might have occurred during the interface generation. Then, the lateral cell vectors are relaxed and equilibrated to the target temperature using the molecular dynamics (MD) method. First, the thermal transport simulation is performed at an average temperature of 500K. The molecular dynamics type is taken as NPT Martyna-Tobias-Kelein [24]. The simulation is carried out for $7X10^4$ steps at log interval of $1.5X10^3$. External stress is switched off and reservoir temperature is set to 500K. In order to remove the center of mass momentum, the initial velocity is set to Maxwell Boltzmann distribution at 500K. These settings are used to carry out the simulation at constant temperature and pressure. When the simulation is done, the grains of the resulting structure is now relaxed and equilibrated at 500K. For the equilibrated structure, regions of the heat source and heat sink are defined within the (200) and (220) oriented grains. The NVT Nose Hoover Chain [25] type MD is then used to equilibrate the system at constant volume. To achieve this, the simulation is carried out for $1X10^5$ steps at log intervals of $1X10^4$ to allow the system to reach steady-state regime. Reservoir and final temperatures are set to 500K, and thermo-state time scale is taken to be 100fs.

Finally, another MD block is used to carry out the non-equilibrium simulations. Here, we set MD type to non-equilibrium momentum exchange, the number of simulation steps and log interval are taken as $8X10^5$ and 2000, respectively. The configuration velocities are used. The time step is set to 1fs. The exchange interval is taken as 200. This is to allow the exchange to stimulate every 200 steps and to increase the transferred kinetic energy per simulation time, which yields larger temperature gradient and a more definite temperature profile. When the simulation is done, the system is carefully checked for convergence with respect to the system size and simulation time. Subsequently, the entire simulation is repeated at other temperatures 600K, 800K and 1000K, respectively

.

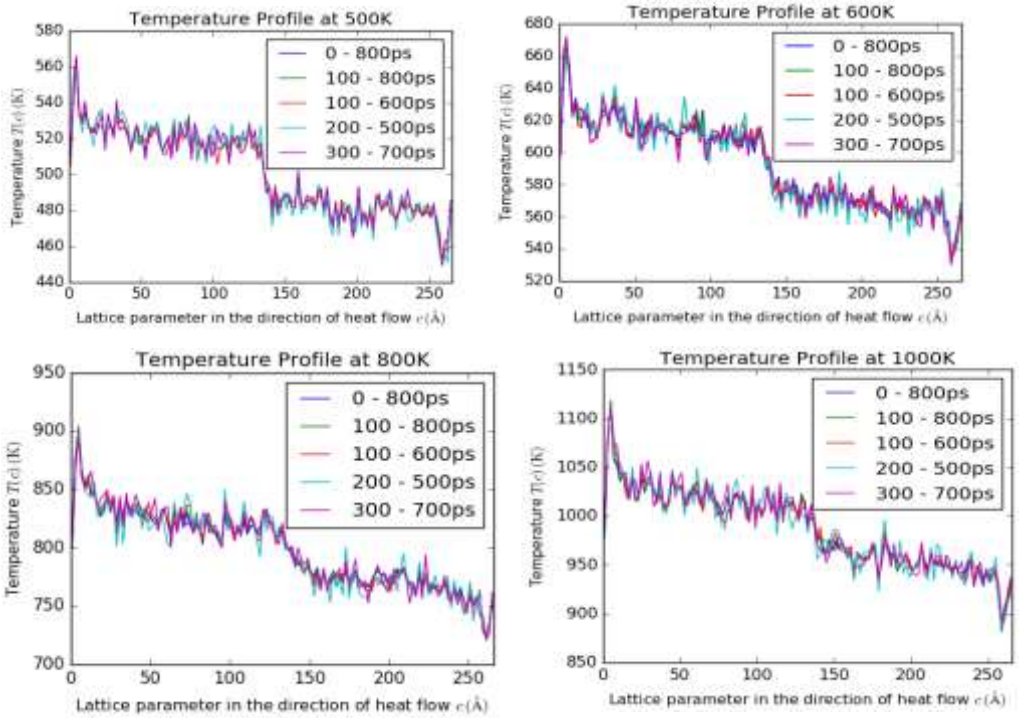

Figure 2. Comparison of temperature profile between 0 - 800ps, 100 - 800ps, 100 - 600ps, 200 - 500ps and 300 – 700ps at different temperatures: 500K, 600K, 800K and 100K.

Result Analysis

First, we check the convergence of the temperature profile with respect to the simulation time. This is done by comparing different time intervals with one another. The temperature profile is shown in Figure 2. The blue, green, red, sky-blue and purple curves correspond to the intervals, 0 – 800 picosecond (ps), 100 - 800ps, 100 - 600ps, 200 - 500ps and 300 – 700ps, respectively. In Figure 2, it can be seen that the curves in the temperature profile are in a steady state. That is, the temperature profile looks the same as time passes. This implies that the temperature profile for 500K, 600K, 800K and 1000K converged with respect to the simulation time. The temperature profile shows positive and negative peaks on the left and right-hand sides of the profile. These areas respectively, signify the heat source and heat sink. This non-linear section comes from the artificial transfer of kinetic energy due to the momentum exchange between the hot and cold grains.

For the system with lattice parameters 11.52X11.52X570, around C_z = 274Å, there is a temperature jump ΔT = 106K. This is the interface region that provides additional thermal resistance. From our simulation, the average heat flux at 500K is 0.00082eV/fs. Therefore, the Kapitza conductance is obtained from Eq. (2.1) as

$$G = \frac{dQ/dt}{\Delta T} = \frac{0.00082 \times \left(1.6 \times 10^{-19} \text{J}\right)}{\left(106\text{K}\right)\left(10^{-15}\text{s}\right)} = 1.2377 \times 10^{-9}\ \text{J/sK or}\ \left(\text{WK}^{-1}\right) \quad (3.1)$$

This implies that the interface between the temperature source and sink causes a discontinuity in the temperature

profile since the interface provides thermal resistance of $R = 1/G$ = 8.0795 X 10^8 KW^{-1}, to the heat current. At 600K, C_z = 276Å and the temperature jump is ΔT = 116K.The average heat flux is obtained as 0.00099eV/fs. Therefore, the thermal or Kapitza conductance is obtained as 1.3655X$10^{-9}$$WK^{-1}$, and the interfacial thermal resistance is 7.3232X$10^8$$KW^{-1}$. Tables 1 – 4 show the average heat flux, temperature jump, Kapitza conductance and interface thermal resistance at different temperatures for the various systems considered. As we can observe, the Kapitza conductance and interface thermal resistance are sensitive to temperature.

Table 1 The Kapitza conductance (G), interface thermal resistance (R), temperature jump (ΔT) and average heat flux (dQ/dt) at different temperatures for (200) oriented grains in the system with lattice parameter 11.52 X 11.52 X 570.

Temperature (K)	C_z(Å)	ΔT(K)	dQ/dt (eV/fs)	G(WK^{-1}) X10^{-9}	R(KW^{-1}) X10^8
500	274	106	0.00082	1.2377	8.0795
600	276	116	0.00099	1.3655	7.3232
800	276	113	0.001272	1.8011	5.5522
1000	275	141	0.001488	1.6885	5.9224

Table 2 The Kapitza conductance (G), interface thermal resistance (R), temperature jump (ΔT) and average heat flux (dQ/dt) at different temperatures for (200) oriented grains in the system with lattice parameter 11.52 X 11.52 X 680.

Temperature (K)	Cz(Å)	ΔT(K)	dQ/dt (eV/fs)	G(WK-1) X10-9	R(KW-1) X108
500	322	122	0.001321	1.7325	5.7720
600	324	168	0.001557	1.4828	6.7439
800	323	186	0.001958	1.6843	5.9372
1000	326	184	0.002478	2.1548	4.6408

Table 3 The Kapitza conductance (G), interface thermal resistance (R), temperature jump (ΔT) and average heat flux (dQ/dt) at different temperatures for (200) oriented grains in the system with lattice parameter 15.3601 X 15.3601 X 270.

Temperature (K)	C_z(Å)	ΔT(K)	dQ/dt (eV/fs)	G(WK^{-1}) X10^{-9}	R(KW^{-1}) X10^8
500	131	79	0.001068	2.1659	4.617
600	132	88	0.001275	2.3213	4.307
800	133	102	0.001688	2.6514	3.771
1000	136	136	0.002167	2.0303	4.925

Table 4 The Kapitza conductance (G), interface thermal resistance (R), temperature jump (ΔT) and average heat flux (dQ/dt) at different temperatures for (200) oriented grains in the system with lattice parameter 15.3601 X 15.3601 X 550

Temperature (K)	C_z(Å)	ΔT(K)	dQ/dt(eV/fs)	G(WK^{-1}) X10^{-9}	R(KW^{-1}) X10^8
500	276	64	0.001036	2.5900	3.8610
600	283	79	0.001237	2.5053	3.9915
800	279	77	0.001635	3.3974	2.9434
1000	279	161	0.002074	2.0611	4.8518

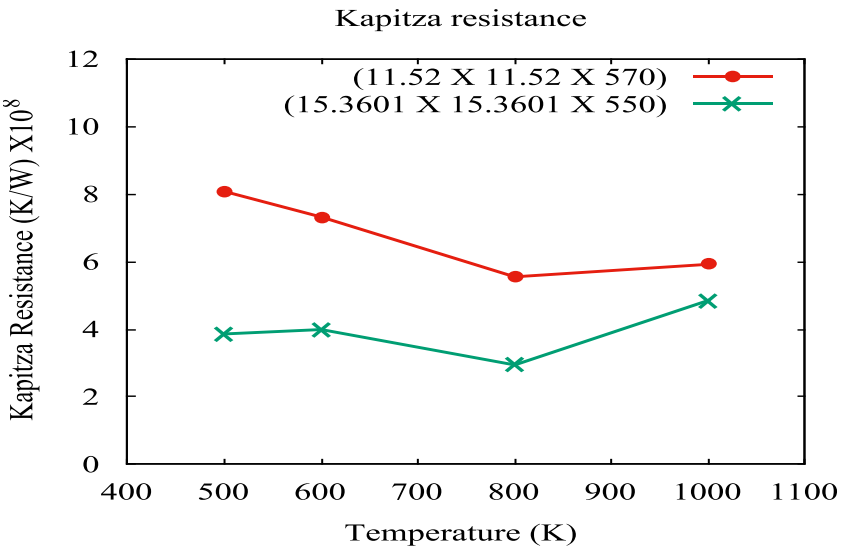

Figure 3. Interface Kapitza resistance as a function of temperature.

Usually, thermal resistance creates a barrier to heat flow leading to temperature jump across the interface [26,27]. Figure 3 displays the interface Kapitza resistance for the supercell crystal 11.52X11.52X570, and 15.3601X15.3601X550, as a function of temperature. As the temperature is increased from 500K to 1000K, the thermal resistance is observed to decrease linearly and then increased for 11.52 X11.52X570. While the interface resistance is observed to first increased as the temperature is increased from 500K to 600k, then decreased at 800K and finally, increased as the temperature is increased to 1000K for the 15.3601X15.3601X550 supercell. This nonlinear behavior is as a result of the difference in discontinuity in the temperature profile at different temperatures. This trend has been obtained earlier by Song and Min [28], who pointed out that interface thermal resistance decreases with temperature in the form , where α is higher for interface with weaker interactions.This significant property of silicon makes it suitable for use as interface material with other semiconductors in integrated circuit applications, with the aim to reduce or increase the thermal resistance across the boundary to allow the desired thermal transport and maintain an appropriate temperature within the electronic device.

Grain Size Dependence of Thermal Conductivity

Also, we calculated the grain size and temperature dependence of the thermal conductivity for the (200) and (220) crystallographic oriented grains. For the various supercells studied, the grain size dependence of the thermal conductivity is tabulated in Tables 5 – 8. Usually, the grain size dependence of thermal conductivity is modeled by the distance between the heat source or sink to the interface boundary. The thermal conductivity κ (W/mK) calculated for different temperatures at

different grain sizes displayed in Figure 4. It is obvious that thermal conductivity is sensitive to both temperature and grain size. For the (200) oriented grains, at each temperature in the four different supercells studied, it is seen that the thermal conductivity increased linearly between grain sizes 116 – 259 Å. Thereafter, there is a jump in thermal conductivity between grain sizes 257 – 270 Å, and then increased linearly again around 317 – 322 Å. A similar trend is also observed for the (220) oriented grains. This might be as a result of boundary effects in the system that is smaller than the mean free path of phonons [29].

Around the (200) oriented grains, at 500K in Tables 5 – 8, for the grain sizes 116, 250, 257 and 317 Å, we obtained the grain thermal conductivity as 29.209, 43.082, 51.18874 and 54.5233 W/mK, respectively. At 600K, for grain sizes 119, 257, 262 and 319 Å, the calculated grain thermal conductivity is respectively, 26.8058, 35.8068, 42.4583 and 47.6362 W/mK. At 800K, the simulated grain thermal conductivity for grain sizes 120, 258, 266 and 320 Å are 22.3884, 28.4109, 30.2294 and 33.1348 W/mK. Finally, at 1000K, for grain sizes 123, 259, 270 and 322 Å, the corresponding grain thermal conductivity is respectively, 15.1379, 18.9584, 22.0628 and 22.0947 W/mK.

Table 5. The grain size, temperature gradient *dT/dz*, and thermal conductivity κ, at different temperatures for (200) and (220) oriented grains in the system with supercell 15.3601 X 15.3601 X 270.

	(200) oriented grains			(220) oriented grains		
Temperature (K)	Grain size (Å)	*dT/dz*(K/Å)	κ(WK^{-1}m^{-1})	Grain size (Å)	*dT/dz*(K/Å)	κ(WK^{-1}m^{-1})
500	116	-0.2483	29.2090	111	-0.2321	31.2477
600	119	-0.3230	26.8058	113	-0.3569	24.2597
800	120	-0.5120	22.3884	115	-0.5851	19.5913
1000	123	-0.9607	15.3179	118	-0.6806	21.6216

Table 6. The grain size, temperature gradient *dT/dz*, and thermal conductivity κ, at different temperatures for (200) and (220) oriented grains in the system with supercell 15.3601 X 15.3601 X 550.

	(200) oriented grains			(220) oriented grains		
Temperature (K)	Grain size (Å)	*dT/dz*(K/Å)	κ(WK^{-1}m^{-1})	Grain size (Å)	*dT/dz*(K/Å)	κ(WK^{-1}m^{-1})
500	250	-0.1633	43.0820	234	-0.1655	42.5093
600	257	-0.2346	35.8067	238	-0.2229	37.6861
800	258	-0.3908	28.4109	242	-0.3533	31.4265
1000	259	-0.7429	18.9584	243	-0.4781	29.4586

Table 7. The grain size, temperature gradient *dT/dz*, and thermal conductivity κ, at different temperatures for (200) and (220) oriented grains in the system with supercell 11.52 X 11.52 X 570.

	(200) oriented grains			(220) oriented grains		
Temperature (K)	Grain size (Å)	*dT/dz*(K/Å)	κ(WK^{-1}m^{-1})	Grain size (Å)	*dT/dz*(K/Å)	κ(WK^{-1}m^{-1})
500	257	-0.1934	51.1874	260	-0.2119	46.7184
600	262	-0.2815	42.4583	262	-0.2902	41.1854
800	266	-0.5080	30.2294	269	-0.4761	32.2548
1000	270	-0.8954	22.0628	272	-0.6774	26.5194

Table 8. The grain size, temperature gradient *dT/dz*, and thermal conductivity κ, at different temperatures for (200) and (220) oriented grains in the system with supercell 11.52 X 11.52 X 680.

	(200) oriented grains			(220) oriented grains		
Temperature (K)	Grain size (Å)	*dT/dz*(K/Å)	κ(WK^{-1}m^{-1})	Grain size (Å)	*dT/dz*(K/Å)	κ(WK^{-1}m^{-1})
500	317	-0.2915	54.5233	317	-0.2440	65.5233
600	319	-0.3946	47.6362	318	-0.3269	57.5014
800	320	-0.7134	33.1348	321	-0.5212	45.3538
1000	322	-1.3540	22.0947	334	-0.6933	43.1505

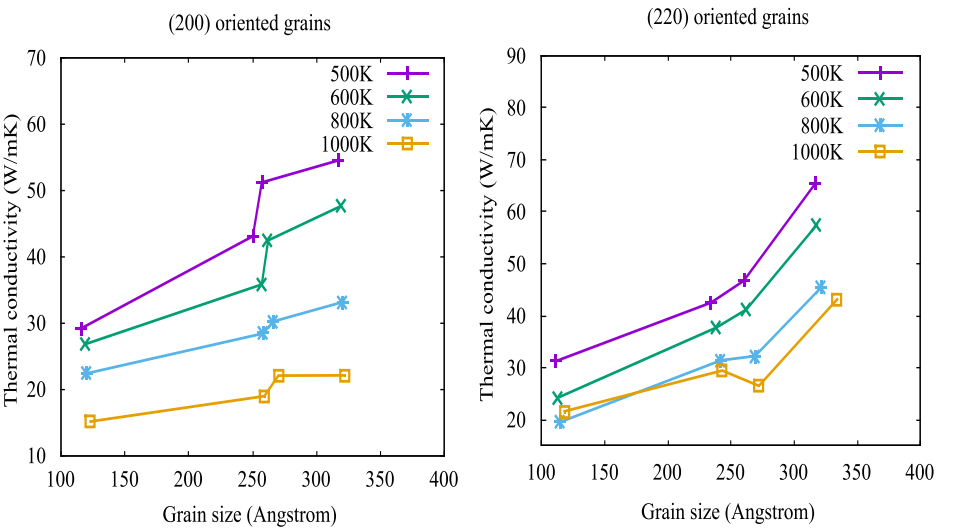

Figure 4. Grain size dependence of the grain thermal conductivity for (200) and (220) oriented grains

In the (220) crystallographic oriented region, the grain sizes considered are 111, 234, 260 and 317 Å at 500K, and the corresponding grain thermal conductivity is 31.2477, 42.5093, 46.7184 and 65.5233 W/mK. At 600K, we obtained 24.2597, 37.6861, 41.1854 and 57.5014 W/mK as the grain thermal conductivity for grain sizes 113, 238, 262 and 318 Å. Around 800K, we calculated 19.5913, 31.4265, 32.2548 and 45.3538 W/mK for grain sizes 115, 242, 269 and 321 Å. Finally, at 1000K, we calculated 21.6216, 29.4586, 26.5194 and 43.1505 W/mK for grain sizes 118, 243, 272 and 334

Å. From the aforementioned, it is clear that, as the grain size is increased, the grain thermal conductivity increased substantially for all grain crystallographic orientation types and temperatures as displayed in Figure 4. The reason for these is that the phonons or lattice waves are scattered near the grain interface. The extent of increase in thermal conductivity is more significant around grain size 317 Å at 500K for both (200) and (220) crystallographic oriented grains, as shown by the purple curve in Figure 4.

It is important to state that results for thermal conductivity obtained from this study are comparably smaller than the bulk thermal conductivity for silicon at 500, 600, 800 and 1000K reported by Howell [30] using the same Stillinger-Weber potential. This trend is expected since the bulk thermal conductivity is generally higher than the corresponding grain thermal conductivity [31]. This is because the mean free path of phonons is normally larger than $1X10^4$ Å, which implies that the simulated smaller grain size suppresses the thermal conductivity [30, 31].

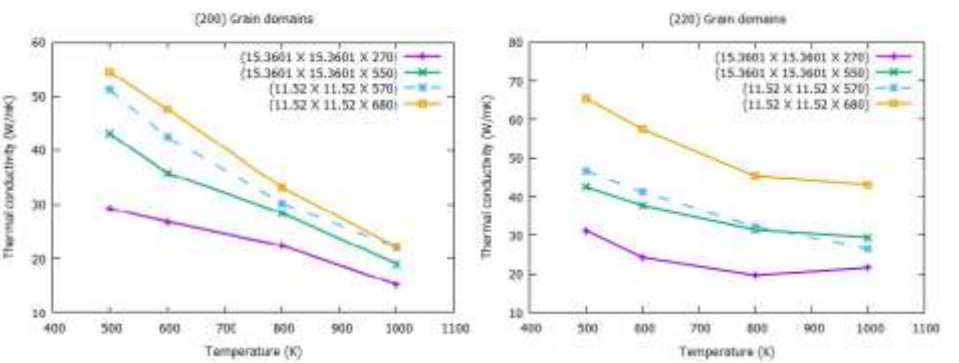

Figure 5. Temperature dependence of the grain thermal conductivity for (200) and (220) oriented grains

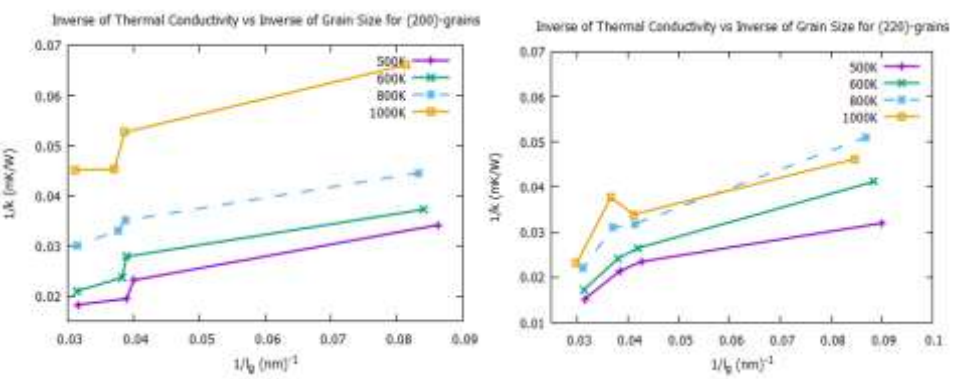

Figure 6. Inverse of thermal conductivity versus inverse of grain size for both (200) and (220) oriented grains.

From Tables 5 – 8, it is also clear that the grain thermal conductivity decreased substantially when the temperature is increased as displayed in Figure 5. These results indicate that simulation size and temperature have

great influence on thermal conductivity of materials, which signifies a positive beneficial effect of grain size and temperature, especially in the micro and nanoelectronic device industries. It is important to note that this behavior has been observed by other researchers using different techniques [32, 33]. Furthermore, Figure 6 displays a plot of the inverse of thermal conductivity against the inverse of grain size. In RNEMD simulations phonons are scattered in the hot and cold regions. Usually, this leads to a lower mean free path, and lower thermal conductivity. It is customary to perform simulations for cells of different sizes to overcome this problem, as has been done by other researchers [34, 35]. Calculating thermal conductivity (κ) for different grain sizes and plotting the inverse of κ against the inverse of lg, it is also possible to extrapolate lg = 0 to determine the thermal conductivity of a simulation of infinite grain size which is comparable to infinite system data [30, 36]. This accounts for the fictitious phonon-boundary scattering introduced by the heat transfer dynamics.

Conclusion

The thermal properties of grain boundaries between Si (200) and Si (220) crystals have been studied by means of reverse non-equilibrium molecular dynamics method. This method allows one to calculate the Kapitza conductance and thermal resistance across the interface, and we found they are both sensitive to temperature. The thermal conductivity monotonically decreased with increasing temperature for all the systems in both crystallographic orientations. We also found that the thermal conductivity is sensitive to the grain size. Increase in grain size resulted in significant increase in thermal conductivity, with the most substantial one around grain size 317 Å at 500K for all crystal orientations. The importance of temperature and grain size effects on thermal properties of crystalline materials is a very vital issue in the micro and nanoelectronic device industries. It is expected that this study will greatly contribute to the full understanding of thermal properties of micro- and nano-crystalline materials.

References

1. Quantumwise Document, www. quantumwise.com.
2. Goddard W. (Ed.), Brenner, D. (Ed.), Lyslevski, S. (Ed.) and Lafrate, G. (Ed.), (2012).andbook of NanoScience, Engineering, and Technology, Third Edition, Boca Raton: CRC Press.
3. Gu, J., Yang, X., Lv, Z., Li, N. Liang, C. Zhang, Q. (2016). Functionalized graphite nanoplatelets/epoxy resin nanocomposites with high thermal conductivity, International Journal of Heat and Mass Transfer 92, 15-22.
4. Simon, R.P. and Alan, J.H.M. (2005). Introduction to Thermal Transport, Elsevier Materials Today, 18 – 20.
5. InternationalTechnology Roadmap for Semiconductors: ITRS Reports, http://www.itrs.net/reports.html.
6. Ferain, I., Colinge, C.A. and Colinge, J. (2011). Multigate transistors as the future of

classical metal–oxide–semiconductor field-effect transistors, Nature, 479, 310 – 316.

7. Schelling, P.K., Shib, L. and Goodson, K.E. (2005). Managing heat for electronics, Mater. Today8 (6), 30-35.
8. Pop, E., Sinha, S. and Goodson, K. E. (2006). Heat Generation and Transport in Nanometer-Scale Transistors, Proceedings of the IEEE, 94 (8), 1587-1601.
9. Haensch, W., Nowak, E.J., Dennard, R.H., Solomon, P.M., Bryant, A., Dokumaci, O.H., Kumar, A., Wang, X., Johnson, J.B. and Fischetti, M.V. (2006). Silicon CMOS devices beyond scaling, IBM Journal of Research and Development, 50, 339-361.
10. Arden L.M., and Li S. (2014). Emerging challenges and materials for thermal management of electronics, Elsevier: Materials Today17 (4), 163 – 174.
11. Datacom Equipment Power Trends and Cooling Applications, 2nd ed., ASHRAE, Atlanta, GA, 2012.
12 na.industrial.panasonic.com/PGS. The Advance Thermal Management Solution for Today's Designs.
13. Tang, B., Hu, G., Gao, H. and Hai, L. (2015). Application of graphene as filler to improve thermal transport property of epoxy resin for thermal interface materials, International Journal of Heat and Mass Transfer,85, 420–429.
14. Siemens, M.E., Li, Q., Yang, R., Nelson, K.A., Anderson, E.H., Murnane, M.M. and Kapteyn, H.C. (2010). Quasi-ballistic thermal transport from nanoscale interfaces observed using ultrafast coherent soft x-ray beams, Nature Mater. 9, 26–30.
15. Müller-Plathe, F. (1997). A simple nonequilibrium molecular dynamics method for calculating the thermal conductivity J. Chem. Phys. 106 (14), 6082-6085.
16. Carlos, N. and Avalos, J.B. (2003). Non-equilibrium exchange algorithm for molecular dynamics simulation of heat flow in multicomponent systems, Mol. Phys. 101 (14), 2303 – 2307.
17. Schelling, P.K. (2004). Kapitza conductance and phonon scattering at grain boundaries by simulation, Journal of Applied Physics,95, 6082 – 6091.
18. Stackhouse, S. and Stixrude L. (2010). Theoretical Methods for Calculating the Lattice Thermal Conductivity of Minerals, Reviews of Mineralogy and Geochemistry, 71, 253-269.
19.Atomistix ToolKit 2017.1, Quantumwise A/S, www.quantumwise.com.
20. Griebel, M., Knapek, S. and Zumbusch, G. (2007). Numerical Simulation in Molecular Dynamics, Springer.
21. Griebel, M. and Hamaekers, J., (2004). Computer Methods in Applied Mechanics and Engineering, 193, 1773-1788.
22. Stillinger, F.H. and Weber, T.A. (1985). Computer Simulation of

local order in condensed phases of silicon, Phys. Rev. B, 31, 5262 – 5271.

23. Zhu, C., Byrd, R.H., Lu, P., and Nocedal, J. (1997). Algorithm 778: L-BFGS-B: Fortran subroutines for large-scale bound-constrained optimization,ACM Transactions on Mathematical Software23 (4), 550 – 560.
24. Martyna, G.J., Tobias, D.J. and Klein, M.L. (1994). Constant pressure molecular dynamics algorithms, J. Chem. Phys., 101 (5):4177–4189.
25. Martyna, G. J., Klein, M. L. and Tuckerman, M. (1992). Nosé–hoover chains: The canonical ensemble via continuous dynamics. J. Chem. Phys., 97 (4), 2635–2643.
26. Kapitza, P.L. (1941). Heat Transfer and Superfluidity of Helium II, Phys. Rev. 60, 354.
27. Robert J.S., Leonid, V.Z. and Norris, P.M. (2007). Effects of temperature and disorder on thermal boundary conductance at solid-solid interfaces: Nonequilibrium molecular dynamics simulations, International Journal of Heat and Mass Transfer,50, 3977–3989.
28. Song, G. and Min, C. (2013). Temperature dependence of thermal resistance at a solid/liquid interface, International Journal at the Interface between Chemistry and Physics,111, 903-908.
29. Nika, D.L., Askerov, A.S. and Balandin, A.A. (2012). Anomalous Size Dependence of the Thermal Conductivity of Graphene Ribbons, Nano Letters 12 (6), 3238–3244.
30. Howell P.C. (2012). Comparison of molecular dynamics methods and interatomic potentials for calculating the thermal conductivity of silicon, J Chem Phys. 137 (22), 224111.
31. Akbar, B., Sang-Pil, K., Rodney, S.R., and Vivek, B.S. (2011). Thermal transport across Twin Grain Boundaries in Polycrystalline Graphene from Nonequilibrium Molecular Dynamics Simulations, Nano Lett., 11, 3917–3921.
32. Sebastian G.V. and Gang C. (2000). Molecular-dynamics simulation of thermal conductivity of silicon crystals, Phys. Rev. B 61, 2651.
33. Mark S.H. and Steven G.L. (1986). Electron correlation in semiconductors and insulators: Band gaps and quasiparticle energies, Phys. Rev. B 34, 5390.
34. Stackhouse, S., Stixrude L. and Karki B.B. (2010), Thermal Conductivity of Periclase (MgO) from first principle, Phys. Rev. Lett. 104, 208501.
35. Patrick K.S, Simon R.P, and Pawel K. (2002). Comparison of atomic-level simulation methods for computing thermal conductivity, Phys. Rev. B 65, 144306.
36. Sellan, D.P., Landry, E.S., Turney, J. E., McGaughey, A.J.H. and Amon, C.H. (2010). Size effects in molecular dynamics thermal conductivity predictions, Phys. Rev. B 81, 214305.